

OPEN ACCESS

EDITED BY
Wei Xiu,
China University of Geosciences, China

REVIEWED BY Xubin Wang, Syracuse University, United States Obey Gotore, Kyushu University, Japan

*CORRESPONDENCE
Lea Hahn

☑ leahahn@uni-koblenz.de

RECEIVED 23 July 2025 ACCEPTED 15 September 2025 PUBLISHED 15 October 2025

CITATION

Hahn L, Vriesen ST, Packroff G, Meier J and Manz W (2025) Anaerobic prokaryotic processes drive manganese release in a drinking water reservoir. Front. Microbiol. 16:1671749. doi: 10.3389/fmicb.2025.1671749

COPYRIGHT

© 2025 Hahn, Vriesen, Packroff, Meier and Manz. This is an open-access article distributed under the terms of the Creative Commons Attribution License (CC BY). The use, distribution or reproduction in other forums is permitted, provided the original author(s) and the copyright owner(s) are credited and that the original publication in this journal is cited, in accordance with accepted academic practice. No use, distribution or reproduction is permitted which does not comply with these terms.

Anaerobic prokaryotic processes drive manganese release in a drinking water reservoir

Lea Hahn^{1*}, Solveig Tabea Vriesen¹, Gabriele Packroff², Jutta Meier¹ and Werner Manz¹

¹Department of Biology, Institute for Integrated Natural Sciences, University of Koblenz, Koblenz, Germany, ²Wahnbach Reservoir Association (Wahnbachtalsperrenverband – WTV), Siegburg, Germany

Introduction: Elevated manganese (Mn) concentrations in drinking water reservoirs present challenges for raw water treatment. During thermal stratification, a shift from oxic to anoxic conditions at the sediment-water interface intensifies the release of dissolved Mn into the water column.

Methods: High-throughput amplicon sequencing of 16S rRNA genes was used to identify the prokaryotic community in sediments of the Wahnbach Reservoir, examining abundance, diversity, and potential metabolic processes concerning key physicochemical parameters. In addition, cultivation-based methods clarified the role of Mn cycling and related biogeochemical processes.

Results: Sediment analyses revealed high sedimentary Mn contents and elevated Mn²⁺ concentrations in pore water. Bioinformatic analysis of 16S rRNA gene sequences revealed a diverse prokaryotic community involved in Mn cycling and competing redox processes, both in sediment samples and enrichment cultures selective for Mn-transforming organisms. Dominant metabolic processes included anaerobic respiration, such as methanogenesis and the reduction of Mn, Fe, sulfate, as well as nitrate, alongside oxidative processes like nitrification and methanotrophy. Cultivation-based approaches confirmed the relevance of these processes and uncovered interconnections among them through the enrichment of specific genera, including *Rhodoferax*, a typical Mn reducer, *Ellin6067*, an ammonium oxidizer, and the methanogen *Methanosarcina*.

Discussion: Seasonal oxygen depletion promotes the release of Mn and Fe from sediments, with Mn(IV) and Fe(III) reduction occurring under increasingly reducing conditions and contributing to metal cycling and redox zonation. This study highlights the dynamic interaction between physicochemical gradients and prokaryotic community structure that drives Mn transformation in stratified freshwater systems.

KEYWORDS

manganese redox cycling, sediment biogeochemistry, 16S rRNA gene sequencing, prokaryotic metabolic processes, drinking water reservoir

1 Introduction

Manganese is an essential trace element crucial for a wide range of metabolic and enzymatic processes across all domains of life (Friedman et al., 2024; Li and Yang, 2018). As the second most abundant trace metal after iron, Mn naturally occurs in oxidation states +II, +III, and +IV (Sujith and Bharathi, 2011). It predominantly exists in solid form, commonly as oxides, carbonates, silicates, or sulfides (Bryant et al., 2012; Ehrlich and Newman, 2008;

LaRowe et al., 2021; Okita and Shanks, 1992; Schaller and Wehrli, 1997). Among these, Mn(IV) (oxyhydr)oxides are particularly reactive, functioning as powerful natural oxidants. They play a key role in redox transformation and, due to their negatively charged surfaces, strongly influence the mobility and bioavailability of trace metals and contaminants by binding metal cations (Godwin et al., 2020; Lovley, 1991; Tebo et al., 2004). In anoxic environments, Mn(IV) (oxyhydr) oxides are reduced either abiotically or via microbial mediation, resulting in the release of soluble Mn²⁺ (Davison, 1993; Giles et al., 2016; LaRowe et al., 2021; Munger et al., 2019).

Microbial Mn(II) oxidation plays a central role in Mn cycling by accelerating oxidation rates by decreasing the activation energy (Carmichael and Bräuer, 2015; Diem and Stumm, 1984; Godwin et al., 2020; Gounot, 1994; Tebo et al., 2004). This process may occur directly via specific proteins or enzymes, such as multicopper oxidases (Corstjens et al., 1997; Gounot, 1994; Kurdi et al., 2022; Tebo et al., 2004; Watanabe et al., 2024), or indirectly through the action of microbially produced oxidants like hydrogen peroxide and free radicals (Carmichael and Bräuer, 2015; Gounot, 1994). Mn(II) can also serve as an electron donor in aerobic respiration, and in combination with CO₂ fixation, it supports a chemolithoautotrophic lifestyle (Gotore et al., 2025; Yu and Leadbetter, 2020). Under anoxic conditions, Mn(IV) minerals are reduced. Given its high redox potential, Mn(IV) acts as a favorable terminal electron acceptor during anaerobic respiration (Davison, 1993). Microorganisms can couple Mn(IV) reduction to the oxidation of organic compounds, methane, ammonium, and sulfide (Godwin et al., 2020; Gounot, 1994; Lovley, 1991; Wang et al., 2022). Overall, microbially mediated Mn redox transformation not only provides energy for microbial metabolism but may also serve protective functions, including shielding against toxic metals, ultraviolet radiation, and reactive oxygen species (Horsburgh et al., 2002; Sujith and Bharathi, 2011).

Redox conditions in freshwater systems, such as lakes and reservoirs, vary considerably across the water column and sediments, with oxygen availability acting as a key driver (Davison, 1993; Lau et al., 2016; Schaller and Wehrli, 1997). During thermal stratification, the development of an anoxic hypolimnion promotes anaerobic microbial processes, leading to the accumulation of dissolved Mn2+ and Fe²⁺, along with the release of other nutrients (Davison, 1993; Lau et al., 2016; Lovley, 1991; Wang et al., 2022). Although Fe is typically more abundant, Mn can reach comparable concentrations under reducing conditions (Canfield et al., 2005). Despite its lower overall abundance, Mn(IV) plays a pivotal role in redox cycling, acting as a key electron acceptor alongside nitrate, Fe(III), and sulfate (Emerson, 2000; Gounot, 1994; Lovley, 1991; Wang et al., 2022; Zhang K. et al., 2022). Importantly, dissolved Mn²⁺ serves as a more sensitive redox indicator than Fe²⁺, as Mn(IV) oxides are reduced at higher redox potentials than their Fe(III) counterparts (Davison, 1993; Sikora et al., 2017).

Dissolved Mn is widespread in water supplies, including reservoirs and groundwater, and frequently exceeds guideline limits set by the World Health Organization (WHO) and the European Drinking Water Directive (European Parliament and Council of the European Union, 2020; Frisbie et al., 2012; WHO, 2021). Elevated Mn concentrations not only cause aesthetic issues, such as a brown discoloration, but also create technical challenges due to the oxidation of Mn²⁺ during water

processing (Li et al., 2022; Tobiason et al., 2016; WHO, 2021; Zhou et al., 2020). In drinking water distribution systems (DWDS), Mn often accumulates as Mn(IV) oxide deposits, which can stimulate biofilm formation and comprise water quality (Li et al., 2022; Zhou et al., 2020). Effective Mn removal requires tailored physical, chemical, or biological treatment strategies adapted to the specific water chemistry and operational conditions of the treatment plant (Tobiason et al., 2016).

The Wahnbach Reservoir, a major drinking water source in North Rhine-Westphalia, Germany, is routinely monitored with high temporal and spatial resolution of the water column to ensure water quality (Herschel, 1995). Over recent decades, shifts in key physicochemical parameters have been documented, affecting both (micro)biological activity and overall biogeochemical cycling within the reservoir (Herschel, 1995; Willmitzer et al., 2015). Notable changes include rising surface water temperatures, earlier and prolonged periods of thermal stratification, less or delayed mixing events, and altered nutrient fluxes (Delpla et al., 2009; Firoozi et al., 2020; Leveque et al., 2021; Willmitzer et al., 2015). During summer stagnation, hypolimnetic measurements revealed declining O2 levels alongside elevated Mn²⁺ concentrations. Despite these observations, the role of sedimentary Mn reservoirs and their interactions with microbial communities remains poorly understood and has received limited scientific attention to date (Herschel, 1995).

This study explores Mn redox cycling in the Wahnbach Reservoir, emphasizing the sediment's dual role as both a source of dissolved Mn²⁺ and a reservoir of Mn(IV) oxides that support Mn-transforming microbial communities at the oxic-anoxic sediment-water interface. Water and sediment core samples were collected from three sampling locations at different water depths and on three sampling dates, capturing a range of redox conditions. Depth profiles of Mn, Fe, and other key parameters were quantified in sediments and pore waters. The prokaryotic community was characterized via 16S rRNA gene amplicon sequencing from both native sediments and enrichment cultures targeting Mn-transforming microorganisms. Enrichments were established using dilution series in selective media, enabling quantification by the most probable number (MPN) method. Microbial metabolisms were inferred from sequence data, and to assess the relative abundance of Mn-transforming prokaryotes, a curated list of 161 relevant genera was compiled.

2 Materials and methods

2.1 Study site and sampling

The Wahnbach Reservoir, located near Siegburg in North Rhine-Westphalia, Germany,¹ served as our study site. Managed by the Wahnbach Reservoir Association (Wahnbachtalsperrenverband – WTV), this reservoir supplies drinking water to over 800,000 residents, primarily drawing from the reservoir itself, with groundwater supplementation. Covering a catchment area of 71.5 km², the area is dominated by over 50% agriculture, 22% forestry, and scattered small residential zones. The reservoir reaches a maximum depth of 46 m, stretches 5.8 km in length, and holds up to

Abbreviations: litMnOx, lithotrophic Mn oxidizers; orgMnOx, organotrophic Mn oxidizers; MnRed, Mn reducers.

¹ https://www.wahnbach.de

41.3 · 106 m3 of water, delivering 80,000 m3 of raw water daily for drinking water production. The primary inflow is the Wahnbach stream, with a phosphorus elimination plant (PEP) located between the pre-dam and the main reservoir. Classified as oligo- to slightly mesotrophic and monomictic, the Wahnbach Reservoir undergoes thermal stratification in summer and mixing beginning in autumn. Sampling was conducted at three sampling locations: buoy A (deepest point near the dam, max. 46 m), buoy E (mid-reservoir, max. 20 m), and buoy H (just behind the pre-dam and PEP, max. 9.5 m) (Figure 1). Raw water extraction occurs at buoy A approximately 2 m above the sediment surface. The WTV routinely monitors physical, chemical, and biological parameters using weekly multiparameter probe measurements, in conjunction with monthly laboratory analyses. The dataset presented here comprises water samples collected in 2022 on July 12, September 13, and October 11 at buoy A, and July 5, September 6, and October 5 at buoy E. Water samples were collected at buoy H only on July 5 as the sampling location could not be reached by boat in September and October due to low water levels. Measurements with a multiparameter probe were conducted the following day. In addition, 1-L water samples (two per buoy and sampling date) were collected in acid-rinsed bottles during regular sampling for subsequent DNA extraction.

Sediment cores were retrieved in July, September, and October 2022 using Corer USC 06000 or USC 09000 (Uwitec GmbH, Mondsee,

A–H: Measuring buoys
PEP: Phosphorus elimination plant

FIGURE 1
Schematic map with top view of the Wahnbach Reservoir. It shows the pre-dam, phosphorus elimination plant (PEP), and measuring

buoys A-H (https://www.wahnbach.de)

AT). On July 14, four cores each were obtained at buoys E and H, and one at buoy A. On September 1, four cores were collected only at buoy A. On October 13, six cores were retrieved at buoy A, four at buoy E, and none at buoy H due to low water level. Immediately after retrieval, redox measurements were performed in one core. The remaining cores were promptly sectioned into 1-cm slices for the upper 4 cm and into 2-cm slices below 4 cm. Cores from buoy A and those from buoy E in October were sectioned to a depth of 16 cm, while all others were processed to 10 cm. Sediment slices were transferred into airtight containers under anoxic conditions using Thermo Scientific™ Oxoid AnaeroGen 2.5-L bags (Thermo Fisher Scientific Inc., Waltham, MA, US), cooled with ice packs, and transported to the laboratory. Subsampling was conducted within 24 h in an anaerobic chamber (Coy Laboratory Products Inc., Grass Lake, MI, US). Pore water was extracted only from buoy A cores (one in September, two in October) by centrifugation outside the anaerobic chamber (3,864 x g, 20 min, 20 °C). Supernatants were immediately returned to the anaerobic chamber and filtered through 0.2-µm membrane filter. Subsamples for DNA extraction were stored at $-80\,^{\circ}$ C, and DNA was extracted from 100–200 mg aliquots within 4 months (July), 17 months (September), and 16 months (October) of sampling. Sediment samples intended for Mn and Fe extractions were stored at −20 °C and processed within one week.

2.2 Physicochemical analysis

In the water column, temperature (°C), pH, and dissolved O₂ (mM, saturation in %) were measured in situ using a multiparameter probe CTD90 (Sea and Sun Technology GmbH, Trappenkamp, DE). Acid-soluble and dissolved Mn and Fe concentrations (µM) were quantified according to DIN EN ISO 11885:2009-09 by inductively coupled plasma optical emission spectroscopy (ICP-OES) using a Varian 720 ES (Varian Inc., Palo Alto, CA, US). Total organic carbon (TOC; μM) was measured following DIN EN 1484:2019-04 by infrared spectroscopy with a DIMATOC® 2000 (Dimatec Analysentechnik GmbH, Essen, DE). Particulate organic carbon (POC; μM) was determined from 1-L water samples filtered through pre-combusted glass fiber filters (GF/C; 480 °C, 4 h), compressed into pellets, and analyzed via combustion at 1,000 °C using a TruSpec® Micro Analyzer (Leco Corporation, St. Joseph, MI, US). Dissolved organic carbon (DOC; μM) was calculated as the difference between TOC and POC. Sulfate (SO₄²⁻; µM) was determined according to DIN EN ISO 11885:2009-09, measured by ICP-OES with a Varian 720 ES (Varian Inc., Palo Alto, CA, US). Nitrite (NO₂⁻; μM) and nitrate $(NO_3^-; \mu M)$ were measured following DIN EN ISO 13395:1996-12, while ammonium (NH₄+; μM) was analyzed according to DIN EN ISO 11732:2005-05, and soluble inorganic phosphate (PO₄³⁻; μM) was determined according to DIN EN ISO 15681-2:2019-05, each quantified by continuous flow analysis (CFA) using a SAN++® Series CFA (Skalar Analytical B. V., Breda, NL).

In sediment samples, the redox potential (Eh; mV) was measured in 1-cm increments using a probe designed and applied according to Geist and Auerswald (2007). To determine the following sediment geochemistry, two cores each from buoys E and H and one core from buoy A were used in July, one core from buoy A in September, and three cores each from buoys A and E in October. Sediment mass density (g mL⁻¹) was determined by weighing 2 mL of fresh sediment

(fresh weight, FW; g). Dry weight (DW; g) and corresponding water content (%) as loss-on-drying (LOD; %; 105 °C, 24 h) were measured. Ash-free dry weight (AFDW; g) was obtained as loss-on-ignition (LOI; %; 519 °C, 5 h) and used to estimate organic matter content. Mn and Fe in sediment samples were extracted using two methods: (i) acid ammonium oxalate (using a solution of 113 mM (NH₄)₂C₂O₄ · H₂O and 87 mM $C_2H_2O_4 \cdot 2H_2O$, pH 3.25) and (ii) dithionite-citrate bicarbonate (using a buffer of 239 mM $C_6H_5Na_3O_7\cdot 2H_2O$ and 200 mM NaHCO₃, ~1 g Na₂S₂O₄ per sample, and a solution of 50 mM MgSO₄ · 7H₂O) (Canfield et al., 1993; Piper et al., 1984). Extracts were diluted in 2% (v/v) HNO₃ and analyzed for Mn and Fe concentrations (mM) by atomic absorption spectrometry (AAS) using an AAnalyst 400 AA Spectrometer equipped with a Lumina[™] hollow cathode lamp (Series N30502XX) (PerkinElmer Inc., Hopkinton, MA, US). Quantification was performed against standards for Mn (Supelco® 1.19789) and Fe (Supelco® 1.19781) obtained from Sigma-Aldrich Chemie GmbH (Taufkirchen, DE). Results were reported in g kg⁻¹_{DW} or mM (mmol L⁻¹ fresh sediment).

In sediment pore water samples, pH was measured immediately after extraction using an inoLab pH 720 pH meter (WTW, Xylem Analytics Germany Sales GmbH & Co. KG, Weilheim, DE). For the determination of dissolved Mn²⁺ and Fe²⁺ (μ M), aliquots were diluted in 2% (v/v) HNO₃ and stored at 4 °C until analysis by AAS. Pore water samples collected in October for the analysis of NO₂⁻ (μ M), NO₃⁻ (μ M), NH₄⁺ (μ M), and PO₄³⁻ (μ M) were stored at –20 °C. Concentrations were measured by a CFA system from Bran+Luebbe GmbH (Norderstedt, DE), comprising multiple AutoAnalyzer 3, XY-3 Sampler, and AutoAnalyzer 3 Digital Colorimeter. Samples for the analysis of SO₄²⁻ (μ M) were also stored at –20 °C and analyzed via ion chromatography (IC) using a 690 IC equipped with a 69 IC pump from Metrohm Deutschland GmbH & Co. KG (Filderstadt, DE).

2.3 Quantification of culturable Mn-transforming microorganisms

To quantify culturable Mn-transforming microorganisms, the most probable number (MPN) technique was applied with a triplicate dilution series of fresh sediment in selective media designed for three functional groups: (i) lithotrophic Mn oxidizers (litMnOx), (ii) organotrophic Mn oxidizers (orgMnOx), and (iii) Mn reducers (MnRed). Mineral medium containing 6 mM KCl, 4 mM NaCl, 1 mM CaCl \cdot 2H2O, 1.9 mM MgCl2 \cdot 6H2O, and 0.1 mM MgSO4 \cdot 7H2O was based on the freshwater medium for sulfate-reducing bacteria (Widdel and Bak, 1992). Vitamin mixture containing thiamine and vitamin B₁₂, non-chelated trace element solution, and selenite-tungstate solution were adapted from Widdel and Bak (1992). A 10 mM 4-(2-hydroxyethyl)-1-piperazineethanesulfonic acid (HEPES) buffer (pH 7.4) was applied. Selective Mn oxidizer media (based on Boogerd and de Vrind, 1987; Okazaki et al., 1997; Stein et al., 2001; Yu and Leadbetter, 2020) contained 2 mM KNO₃ and 0.3 mM KH₂PO₄ as N and P sources, respectively, with freshly prepared Mn carbonate as Mn(II) source (~80 mM for litMnOx and ~20 mM for orgMnOx). Medium for organotrophic Mn oxidizers was additionally enriched with 0.5 g L⁻¹ yeast extract, 0.5 g L⁻¹ casamino acids, and 5 mM D(+)glucose · H₂O. Mn reducer medium (adapted from Lovley, 2006; Lovley and Phillips, 1988; Vandieken et al., 2012) contained additionally 5 mM NH₄Cl, 1.5 mM KH₂PO₄, 5 mM Na-acetate, 5 mM Na-lactate, and \sim 14 mM freshly prepared Mn oxide as Mn(IV) source.

MPN dilution series were conducted for selected sediments from three depth intervals (0-2 cm, 2-4 cm, 8-10 cm) collected from the three sampling locations in July and October (Supplementary Table S3). The sediment samples were homogenized over the corresponding depths and, where available, pooled from multiple cores to ensure representative sampling. Initial dilutions were prepared in 100-mL sterile serum bottles containing 45 mL of selective medium and 5 mL of sediment (10% v/v). Serial dilutions were subsequently performed in 20-mL serum bottles (10-fold in July: 1 mL sediment slurry + 9 mL medium; 5.5-fold in October: 1 mL sediment slurry + 4.5 mL medium). After inoculation, Mn oxidizer bottles were sealed with sterile parafilm, while Mn reducer bottles were sealed with sterile butyl rubber stoppers. The headspace of the Mn reducer bottles was sparged with N₂/CO₂ (80:20 v/v) gas mixture to create anoxic conditions. All cultures were incubated at 20 °C. Mn oxidation is indicated by brown coloring, and Mn reduction by discoloration (Krumbein and Altmann, 1973; Wendt-Potthoff et al., 2014). MPN evaluation was carried out six weeks after inoculation using the EPA MPN Calculator (https:// mostprobablenumbercalculator.epa.gov/mpnForm, version U. S. Environmental Protection Agency, Washington, DC, 2013).

2.4 DNA extraction

For DNA extraction from MPN cultures, aliquots of 9 mL (July) and 4.5 mL (October) were taken from selected dilutions (Supplementary Table S3) after 15 weeks and 9 weeks of incubation, respectively. Microbial cells were harvested from culture liquid by centrifugation (4,153 x g, 10 °C, 20 min) and stored at −80 °C until further processing. DNA extractions were carried out 1 month (July) and 14 months (October) after sampling. Genomic DNA from both MPN enrichment cultures and sediment samples was extracted using the DNeasy PowerSoil Kit from Qiagen GmbH (Hilden, DE). For water samples, 1-L aliquots were filtered on the day of sampling using 0.2-µm cellulose acetate filters, which were immediately frozen at -80 °C and later processed using the DNeasy PowerWater Kit (Qiagen GmbH, Hilden, DE). DNA concentrations (nM) were measured using the Qubit dsDNA BR Assay Kit in combination with a Qubit 4 Fluorometer (Invitrogen by Thermo Fisher Scientific, Waltham, MA, US). All extracted DNA was stored at -80 °C for subsequent molecular analyses.

2.5 Sequencing and bioinformatic analysis

Bacterial community composition was assessed by targeting the V3-V4 region of the 16S rRNA gene. Amplicon Sequencing was conducted by Novogene Europe (Cambridge, UK, https://www.novogene.com/eu-en/) using the primers 341F (5'-CCTAYGGGRB GCASCAG-3') and 806R (5'-GGACTACNNGGGTATCTAAT-3'). Libraries were sequenced on an Illumina NovaSeq 6000 platform (San Diego, CA, US) to generate 250 bp paired-end raw reads. Sequence analysis was performed by Novogene using the bioinformatics pipeline QIIME (Quantitative Insights Into Microbial Ecology). For the July samples, raw sequences were analyzed using QIIME1 (http://qiime.org/index-qiime1.html, version 1.9.1), with sequences clustered into operative taxonomic units (OTUs) at ≥97% similarity. Further analysis

of phylogenetic relationships and dominant taxa was conducted using Uparse software (http://drive5.com/uparse/, Uparse v7.0.1001, Edgar, 2013), and multiple sequence alignment was performed using MUSCLE software (http://www.drive5.com/muscle/, version 3.8.31, Edgar, 2004). Taxonomic annotation was based on the SILVA Database (http://www.arbsilva.de/, SILVA138, Quast et al., 2013) using the Mothur algorithm. For the September and October samples, sequence processing was performed using QIIME2 (https://qiime2.org/, version QIIME2-202202), employing DADA2 (Callahan et al., 2016) for denoising and generating amplicon sequence variants (ASVs). Unlike OTU-based approaches, ASVs are resolved at 100% sequence similarity, using QIIME2's classify-sklearn algorithm (Bokulich et al., 2018; Bolyen et al., 2019), a pre-trained Naive Bayes classifier, and the SILVA Database (SILVA138).

Major microbial metabolisms were identified using FAPROTAX (Functional Annotation of PROkaryotic TAXa; https://pages.uoregon. edu/slouca/LoucaLab/archive/FAPROTAX/lib/php/index.php, version 1.2.10, Louca et al., 2016). This tool assigns functional and metabolic traits to taxa based on curated taxonomic classifications linked to experimentally characterized strains and their known physiology from the literature. Functional assignments were generated using the collapse_table.py script, taking OTU or ASV tables as input. The script was executed using Python (https://www.python.org/psf-landing/, version 3.11.2, Python Software Foundation, Wilmington, DE, US) managed through miniconda3. Our analysis focused on key aerobic and lithotrophic processes (methanotrophy, nitrification, oxidation of sulfur compounds, Fe oxidation, and Mn oxidation) as well as on anaerobic respiration pathways (methanogenesis and respiration of nitrate, sulfate, Fe, and Mn). In the July sequencing dataset, 15.0% of all sequences were assigned to at least one functional or metabolic annotation of all processes compiled in FAPROTAX, and in the October sequence batch, 22.1% of the sequences were assigned. To enhance the resolution of Mn-transforming groups, we curated a comprehensive list of 161 prokaryotic genera associated with Mn cycling, compiled from an extensive literature research covering 235 articles (Supplementary Table S8).

Point and bar charts were created using Microsoft Excel LTSC MSO (16.0.14332.20824, Microsoft Corporation, Redmond, WA, US). Bubble plots, heatmaps, and, for advanced multivariate analyses, non-metric multidimensional scaling (nMDS) plots were generated with R (version 4.4.22024-10-31 ucrt, R Foundation for Statistical Computing, Vienna, AT) within R Studio (2024.12.0 Build 467, Posit Software, PBC, Boston, MA, US), employing the widely used "vegan" package (Oksanen et al., 2025) for ecological ordination and "ggplot2" (Wickham, 2016) for data visualization. To illustrate the core microbiota patterns in sediments, MPN cultures, and across the three sampling locations (buoys A, E, and H), ellipses representing 95% confidence intervals were drawn using a multivariate t-distribution (type = "t," level = 0.95), providing a robust visualization of community clustering and variability.

3 Results

3.1 Physicochemical gradients in the water column

Surface temperatures peaked at 22.9–23.5 $^{\circ}$ C in July and September, dropping to 15.4–16.5 $^{\circ}$ C in October

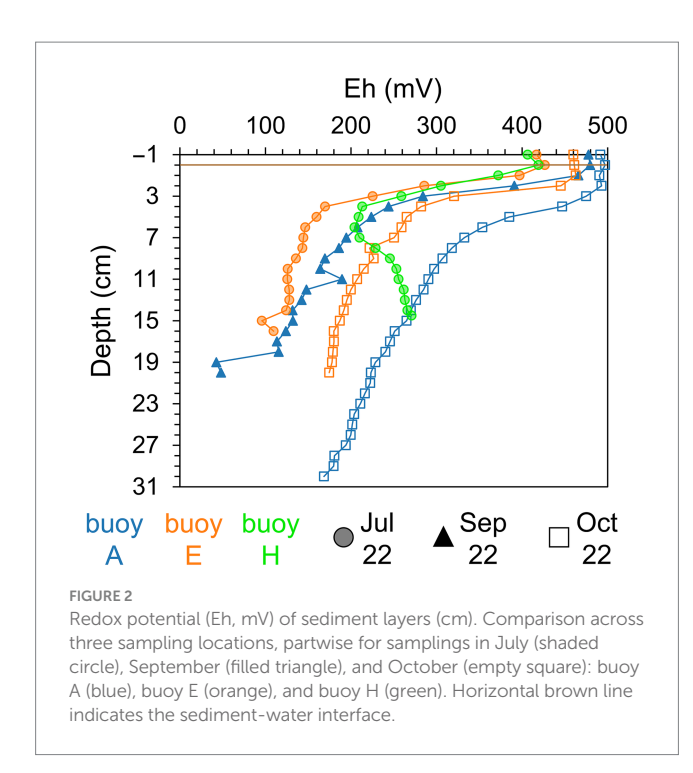
(Supplementary Figure S1). Thermal stratification developed at buoys A and E, with epilimnion depths of 6–7 m in July and September, respectively. Bottom water temperatures ranged from 6.4–7.0 °C (buoy A) to 8.1–12.0 °C (buoy E). O₂ oversaturation occurred near the thermocline with up to 472 μ M O₂ (buoy A), but O₂ levels declined sharply toward the sediment, reaching 69 μ M (buoy A, October) and 3 μ M (buoy E, September). The corresponding pH values ranged from alkaline in surface waters (8.0–8.9) to more acidic near the bottom (6.6–6.8). Remarkably, acid-soluble Mn was elevated in bottom waters, up to 9.4 μ M at buoy A and 24.1 μ M at buoy E, with dissolved Mn²+ contributing up to 83% (buoy A). Fe enrichment was observed only at buoy E in September/October (up to 5.9 μ M). Mn consistently exceeded Fe by factors of up to 47 (buoy A) and 8 (buoy E). Buoy H showed no stratification or Mn and Fe enrichment.

POC remained lower than DOC at all sampling locations and sampling dates. POC ranged from 5.2–36.8 μM (buoy A), 24.0–71.0 μM (buoy E), and 42.7–49.6 μM (buoy H). DOC generally decreased with depth, but occasionally increased near sediments. Surface DOC was 147.9–212.4 μM , dropping to 101.7–143.2 μM (buoy A) and 110.2–166.0 μM (buoy E). Near the surface, SO₄ 2 - was highest with 242.6–253.0 μM , with one notable peak at buoy H (803.7 μM , July). Values for PO₄ 3 - remained very low ($\leq 0.06 \, \mu M$). Surface NO₂- peaked at 0.9–1.3 μM , decreased with depth, but increased again near sediments at buoys A and E. In surface layers, NO₃- ranged from 129.0–169.3 μM , peaking at 208.0 μM (buoy A) before declining near the sediment. Concentrations of NH₄+ remained low throughout (0.3–3.4 μM), but rose near the sediment to 12.2 μM (buoy A) and 7.2 μM (buoy E). DNA concentrations were used as a proxy to indicate (microbial) biomass and showed spatial variation.

3.2 Geochemical characteristics in the sediment and pore water

Sediment color and texture, as determined by visual inspection, varied both spatially and vertically across sampling locations. At buoy A, surface sediments were brown to rust-colored and fluffy, transitioning to dark gray or black, loamy sediments with depth. Sediments at buoy E had a firmer brown surface, becoming dry, compact, and black deeper down. At buoy H, sediments were sandy, brownish with plant debris and increasingly darker zones indicative of organic matter accumulation. Redox potential profiles (Figure 2) showed strong stratification. Oxic conditions (>300 mV) were present in the overlying water and upper 2-3 cm of sediment across all sampling locations. Below this, redox potential declined sharply within 1-5 cm, marking the transition to anoxic conditions (<300 mV). At buoys A and E, redox values in sediment continued decreasing with depth. In contrast, redox potential in sediments at buoy H showed a minimum followed by a rise at depth. A seasonal redox shift toward more oxidizing conditions at depth was observed from summer to autumn, particularly in sediments at buoy E (July to October) and buoy A (September to October).

Water content across sediment profiles showed clear spatial and temporal variation (Supplementary Figure S2A). In sediments at buoy A, water content was high (67–90%) but dropped locally to 53–58% at 2–4 cm depth in July. That same month, surface sediments at buoys E and H had similarly high water content but declined more steeply with depth, reaching 37–53% in deeper



layers. In October, water content ranged from 61 to 87% in sediments at buoys A and E, with consistently lower values at depth at buoy E. Organic matter content, assessed as AFDW, showed distinct depth trends (Supplementary Figure S2B). At buoy A in July, surface organic content in sediments peaked at 15%, declined to 3.5% at 2–4 cm, and then rose again to 7–9% in deeper layers. Sediments at buoys E and H showed a more gradual decrease of organic matter with depth (5–9%), with sediments at buoy H maintaining consistently higher values. In September, organic matter in sediments at buoy A reached 11% at 2–3 cm, while deeper layers stayed similar to July. By October, organic content in sediments at buoys A and E ranged from 5 to 8% throughout the profile.

Dithionite-extractable Mn reached the highest concentrations in sediments at buoy A (10-28 mM), far exceeding levels at other sampling locations (Figure 3A). In July, Mn increased slightly with depth, while in September and October, peak values were confined to the upper 2-3 cm. Sediments at buoy E showed moderate Mn concentrations (5-11 mM) with notable core-to-core variability in deeper layers. At buoy H, sediments exhibited consistently the lowest Mn levels (1-5 mM), with higher concentrations at greater depths. Dithionite-extractable Mn was generally comparable to oxalate-extractable Mn, except at depth, where oxalate-extractable Mn prevailed (Supplementary Figure S3A). Fe concentrations exceeded Mn at all sampling locations and depths, except in the surface sediment layers at buoy A (Figures 3B and Supplementary S3B). Dithionite-extractable Fe in sediments at buoy A ranged from 21 to 70 mM, the lowest among the sampling locations, while sediments at buoys E and H showed higher values (60-121 mM and 62-125 mM, respectively), typically increasing with depth. At buoy A, Fe concentrations in sediments were up to 5.5-fold higher than Mn; in sediments at buoys E and H, Fe exceeded Mn by factors of 6-25 and 18-59, particularly in deeper layers. Oxalate-extractable Fe was slightly higher than dithionite-extractable Fe, especially at depth. A complementary representation of Mn and Fe depth profiles in g kg⁻¹_{DW} is provided in Supplementary Figure S4.

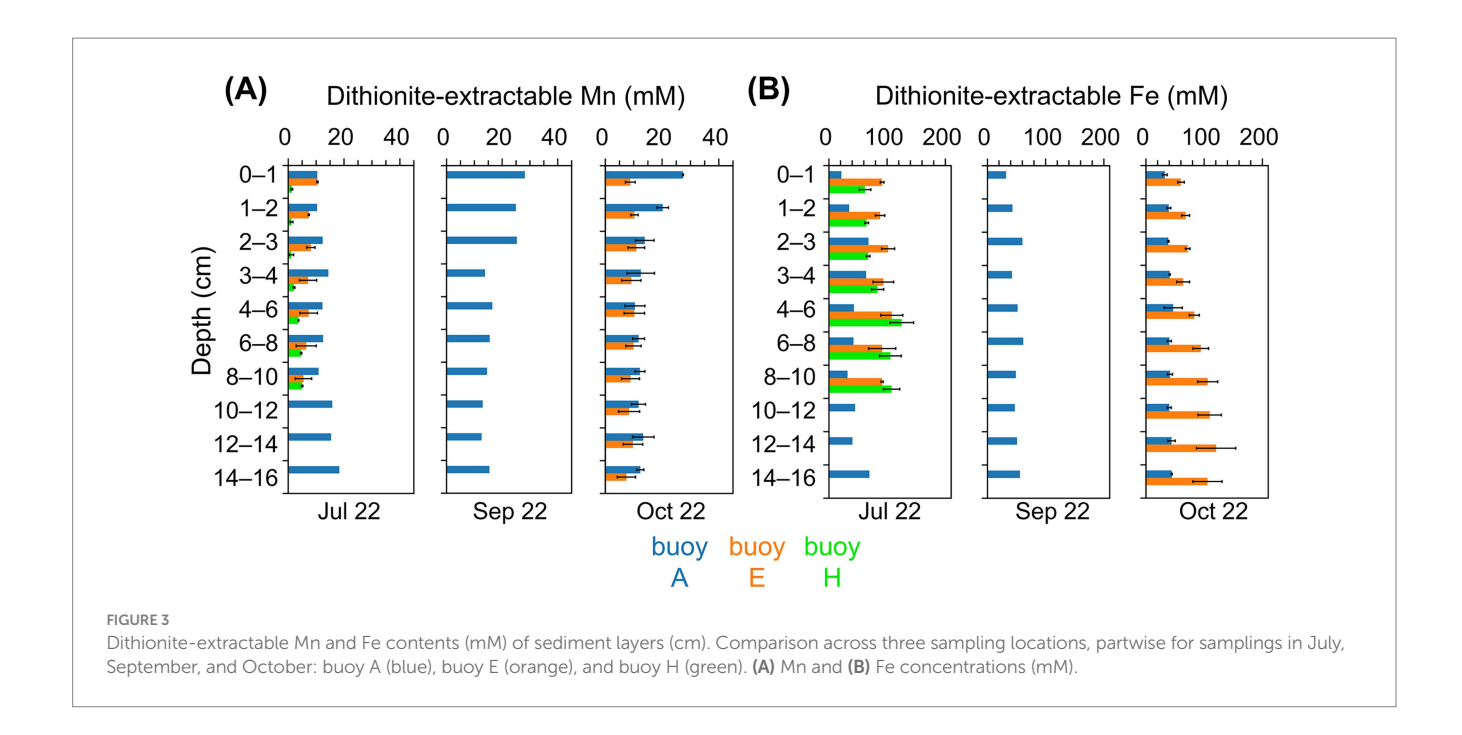
Pore water analysis at buoy A (Figure 4) from September and October showed pH values of 6.9–7.9, slightly increasing with depth. Dissolved Mn²+ and Fe²+ concentrations increased with depth, peaking at 276 μM (Mn) and 196 μM (Fe) in September. Mn²+ consistently exceeded Fe²+, indicating Mn as the dominant redox-active metal. In October, NO₂- and NO₃- remained low (~0.4 μM and ~0.8 μM), while NH₄+ and PO₄³- increased with depth, reaching up to 127 μM and ~1.7 μM , respectively. In contrast, SO₄²- sharply declined from 438 μM in the upper 5 cm.

3.3 Prokaryotic community composition and metabolisms in the sediment

The ten most abundant prokaryotic classes across sediment samples Gammaproteobacteria, Alphaproteobacteria, Vicinamibacteria, Bacteroidia, Bacilli, Clostridia, Methanosarcinia, Thermoleophilia, KD4-96, and Verrucomicrobiae, comprising 42.3-72.4% of total sequences (Supplementary Figure S5). Their distribution varied by sampling location and sampling date. Clear depth profiles were evident, with Gammaproteobacteria more abundant in surface sediments, while Bacilli, Clostridia, and Methanosarcinia prevailed in deeper layers, reflecting a shift toward anaerobic taxa. Gammaproteobacteria, the most abundant class, is metabolically diverse (Liu Q. et al., 2022; Liu W. et al., 2018; Newton et al., 2011; Song et al., 2024; Wu et al., 2017; Zemskaya et al., 2021). Bacilli and Clostridia form endospores and persist under unfavorable conditions; Clostridia contribute to anaerobic degradation of organic polymers and fermenting degradation products (Dürre, 2015; Huang et al., 2017; Song et al., 2024; Wu et al., 2017). Notably, Methanosarcinia were relatively abundant in the Wahnbach Reservoir as a class of methane-producing Archaea (Ji et al., 2016; Zemskaya et al., 2021). Alphaproteobacteria, Vicinamibacteria, Bacteroidia, Thermoleophilia, KD4-96, and Verrucomicrobiae showed no clear depth-related distribution patterns.

The nMDS plots (Figure 5) revealed distinct compositional differences and a clear clustering of prokaryotic communities by sampling location, as well as a gradient related to sediment depth. Communities in sediments at buoys A and E were more similar to each other. Those at buoy H, particularly in deeper sediments, were clearly divergent. The sediment depth-related gradient, most notably at buoy A (July and October) and buoy H (July), reflected the vertical stratification of microbial assemblages. The greatest similarities between the different sampling locations were found in the upper sediment layers; accordingly, deeper sediment layers increasingly differed.

The depth-resolved distribution of the key oxidizing and reducing metabolisms of interest, predicted by FAPROTAX and supplemented by our curated list of Mn-transforming genera (based on an extensive literature research), is presented in Figure 6, with dominant genera listed in Supplementary Tables S1, S2. Metabolic processes and associated prokaryotes are presented according to their relative abundance in FAPROTAX, starting with oxidizing processes, and concluding with a detailed description of the Mn-transforming organisms (Figure 6, Supplementary Tables S1, S2).



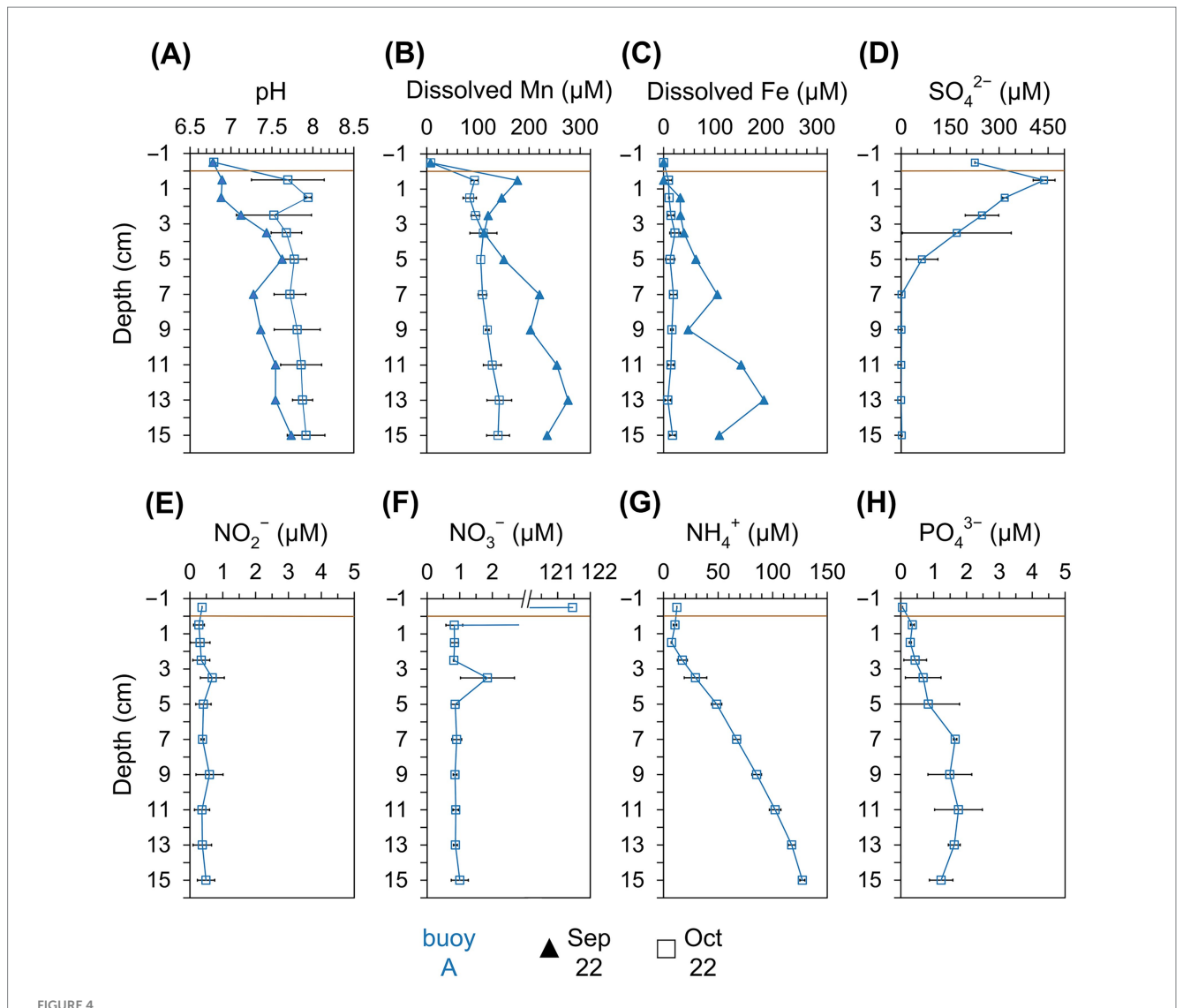
Methanotrophy (0.2–7.1%) was consistently present in sediments at all sampling locations, with the highest levels observed in surface sediments (0-2 cm) and declining with increasing depth. Key methanotrophs included "Candidatus Methylomirabilis", Crenothrix, Methylobacter, and Methylocystis. The latter is capable of anoxic methane oxidation via nitrate reduction (Cheng et al., 2017; Su et al., 2022; Vigliotta et al., 2007). Nitrification was the most abundant process (up to 18.1%), highest in surface layers at buoy A, and decreased with depth. Dominant nitrifiers included Ellin6067, GOUTA6, and MND1. Next to Ellin6067, the typical nitrifier Nitrospira was detected, also noted as a potential Mn oxidizer (Laanbroek and Bollmann, 2011; Miyata et al., 2024; Palomo et al., 2016; Wang et al., 2014). Sulfur compound oxidation (up to 1.4%) was mainly detected in deeper sediments at buoy H, dominated by Thiobacillus. Fe oxidation was sporadic and low (≤0.6%), with Gallionella as the main genus. FAPROTAX-predicted Mn oxidation was rare (≤0.04%) and mostly absent; only *Pedomicrobium* was consistently assigned.

Literature research revealed higher Mn-oxidizer abundances (1.2-9.5%), decreasing with sediment depth at buoy A but stable at buoys E and H. Prominent genera included Nitrospira, Crenothrix, Arenimonas, and Hyphomicrobium, indicating greater diversity than captured by standard functional annotation tools. Most of these species are known to oxidize other reduced inorganic compounds: Nitrospira oxidizing NH₄⁺, NO₂⁻, and Fe(II) (Cai et al., 2023; Mehrani et al., 2020; Palomo et al., 2016), Crenothrix oxidizing NH₄+, CH₄, and Fe(II) (Cai et al., 2023; Cheng et al., 2017; Sujith and Bharathi, 2011; Vigliotta et al., 2007), and *Hyphomicrobium*, oxidizing CH₄ and Fe(II) (Kurt, 2019; Sujith and Bharathi, 2011; Vuilleumier et al., 2011). Arenimonas are linked to metal(loid) immobilization via biosorption and mineral formation (Liu J. et al., 2018). Further commonly reported Mn oxidizers, such as Leptothrix, Pedomicrobium, and Arthrobacter (Cai et al., 2023; Carmichael and Bräuer, 2015; Ehrlich and Newman, 2008; Gounot, 1994), were less abundant or absent in the sediments of the Wahnbach Reservoir.

Methanogenesis was consistently present in sediments at all sampling locations and dates, with the highest relative abundances (up to 9.6%) in deeper sediments, particularly at buoy A. Methanoregula and Methanosarcina were the dominant genera. Although less abundant, Methanosarcina species are known to oxidize methane coupled to Mn(IV) reduction (Chen et al., 2023; Ji et al., 2016; Liu et al., 2020). Nitrate respiration showed low relative abundances (\leq 1.2%), with *Dechloromonas* as the main taxon. Sulfate respiration was more abundant (up to 3.0%), driven by Sva0081 sediment group, Desulfatiglans, and Desulfatirhabdium. Sulfate respiration occurred in deeper sediment layers. Sequences related to Desulfobulbus, Desulfobacterium, and Desulfobacterium (Holmer and Storkholm, 2001) were less abundant. Notably, Desulfobulbus can also reduce Mn(IV) (Lovley and Phillips, 1994). Fe respiration was low (\leq 0.4%), primarily involving *Desulfuromonas* and *Geobacter*. Mn respiration, as annotated by FAPROTAX, appeared only in three samples at \leq 0.01%, and was only represented by the genus *Geobacter*.

Using the list of Mn reducers from our literature research, much higher relative abundances (1.1-8.7%) were found, especially in deeper sediment layers at buoy E, followed by buoy H. Key Mn-reducing genera included Clostridium, Anaeromyxobacter, Paenibacillus, and "Candidatus Methanoperedens". Clostridium is mainly fermentative but also capable of metal reduction (Francis and Dodge, 1991; Lovley, 1991; Pyne et al., 2014; Shoiful et al., 2020), and Anaeromyxobacter is known for CH₄ and NH₄⁺ oxidation and dissimilatory metal-reduction (Liu et al., 2023; Liu et al., 2020; Wang et al., 2020). Paenibacillus is associated with N₂ fixation, PO₄³⁻ solubilization, and Fe(III) reduction (Ehrlich and Newman, 2008; Grady et al., 2016). The archaeon "Candidatus Methanoperedens" oxidizes CH₄ coupled to NO₃⁻ and Fe(III) reduction (Leu et al., 2020; Liu et al., 2020; Su et al., 2020). Other known Mn reducers, including Geothrix, Geobacter, and Rhodoferax (Coates et al., 1999; Finneran et al., 2003; Liu et al., 2023; Lovley et al., 1993), were present in lower abundances in the sediments of the Wahnbach Reservoir.

Prokaryotes with Mn-reducing and/or -oxidizing capacity, identified through our literature research, were widespread across all sampling



Physicochemical parameters in the pore water retrieved from different sediment layers (cm). Comparison across the sampling location of buoy A (blue) for samplings in September (filled triangle) and October (empty square). (A) pH, (B) dissolved Mn (μ M), (C) dissolved Fe (μ M), (D) SO₄²⁻ (μ M), (E) NO₂⁻ (μ M), (F) NO₃⁻ (μ M), (G) NH₄⁺ (μ M), and (H) PO₄³⁻ (μ M). Horizontal brown line indicates the sediment-water interface.

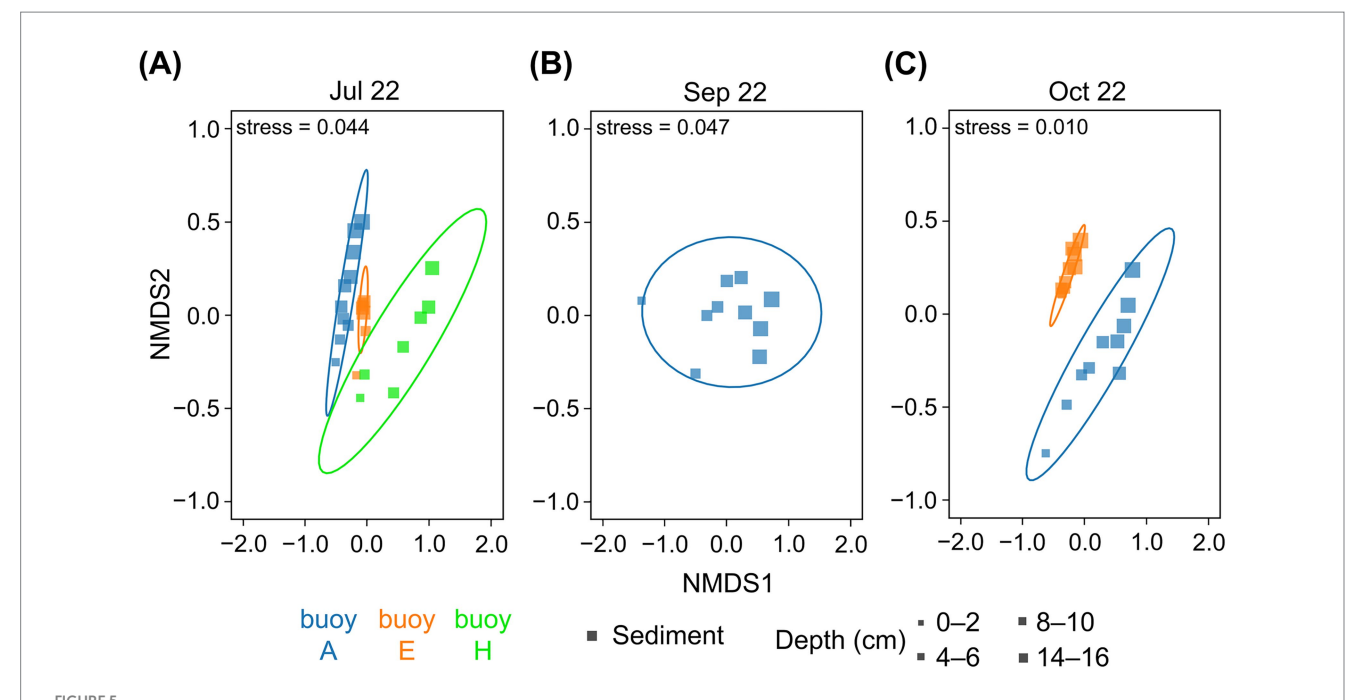
locations, depths, and sampling dates, comprising 2.1–25.0% of the community, with *Bacillus* and *Ellin6067* as dominant taxa. *Bacillus* use organic compounds in aerobic respiration and can affect metal cycling through biosorption, metal cation oxidation, and metal oxide reduction (Francis et al., 2002; Kanso et al., 2002), and *Ellin6067* is known to couple NH₄⁺ oxidation to Mn(IV) reduction (Jiang Z. et al., 2024; Liu et al., 2023). Other Mn-transforming genera, such as *Shewanella* and *Pseudomonas* (Cai et al., 2023; Gounot, 1994; Lovley, 1991), were less abundant or absent in the sediments of the Wahnbach Reservoir.

3.4 Most probable number (MPN) of Mn-transforming microorganisms and community composition of selected cultures

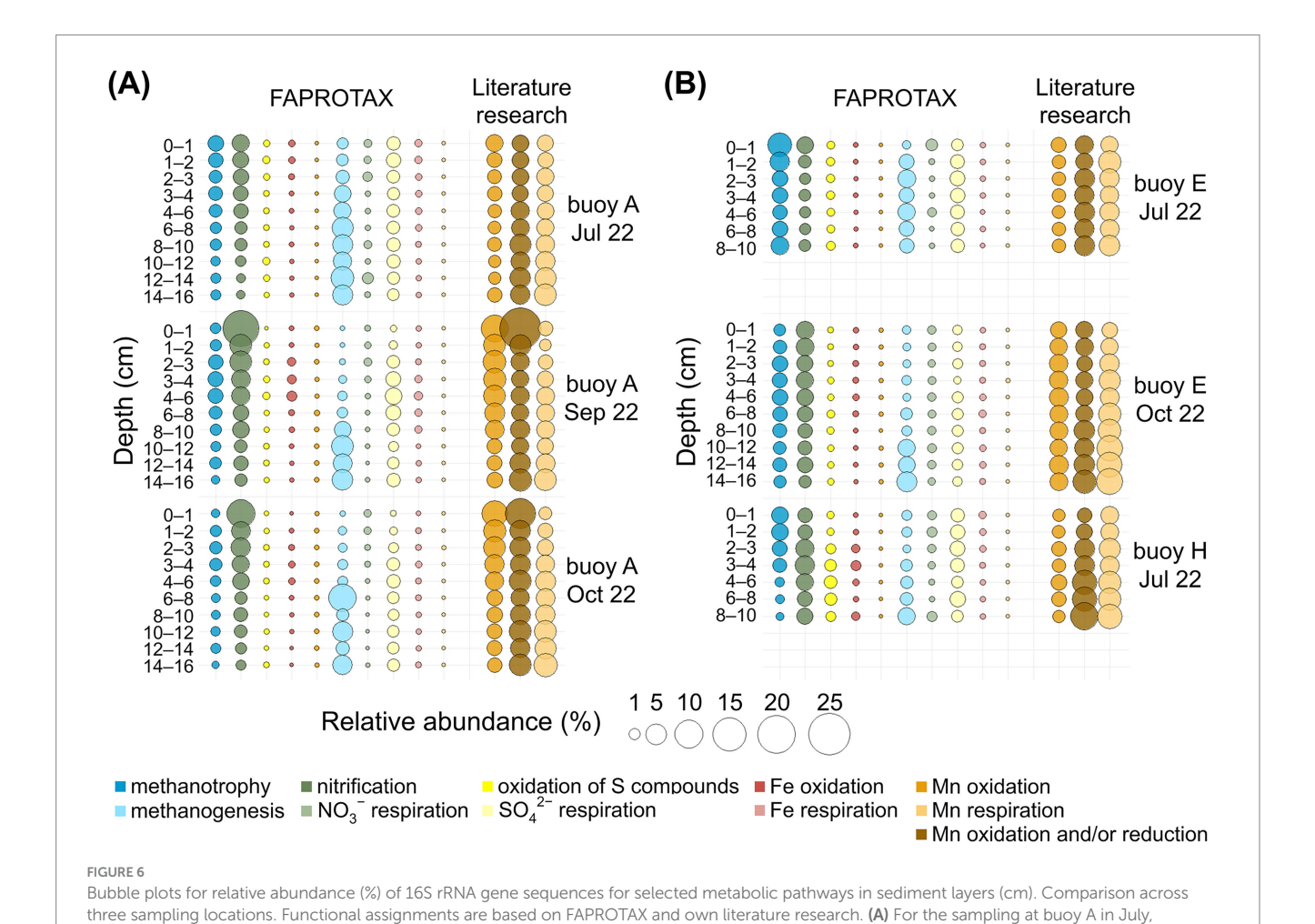
The culture-based approach provided semi-quantitative estimates of active Mn-transforming microbes (Supplementary Table S4). No

visible brown coloration developed during the six-week incubation, indicating the absence of detectable lithotrophic Mn oxidizers under the tested conditions. Organotrophic Mn oxidizers were initially scarce (<100 cells mL^{-1} in July) but increased notably by October, reaching 10^3-10^5 cells mL^{-1} at buoys A and E, with a maximum of 5.6 \cdot 10^4 cells mL^{-1} in surface sediments at buoy A. Mn-reducing prokaryotes were more abundant overall (10^2 to 10^5 cells mL^{-1}), particularly at buoys E and H in July, peaking at $4.3 \cdot 10^4$ cells mL^{-1} in surface sediments at buoy H.

The nMDS plots illustrate patterns of similarity and divergence between prokaryotic communities from enrichment cultures and the original sediment samples. Communities enriched in cultures of lithotrophic Mn-oxidizing microorganisms were generally similar to one another, resembling those of the original sediments, especially in October (Supplementary Figures S6A,B). 16S rRNA gene sequencing identified *Ellin6067*, *Labrys*, MND1, and *Caulobacter* as dominant genera (Figures 7A,B, Supplementary Table S5). Among these, *Ellin6067* and MND1, both abundant in sediments, are known



The nMDS plots of OTU/ASV distribution of sediment core samples based on 16S rRNA gene sequences. Comparison across the three sampling locations of buoy A (blue), buoy E (orange), and buoy H (green). Symbol size represents sediment depth (cm). Sediment samples (square) from (A) July, (B) September, and (C) October. Core microbiota indicated by ellipses based on multivariate t-distribution with a 95% confidence interval. Stress values are provided.



nitrifiers, though only *Ellin6067* has been linked to Mn cycling (Jiang Y. et al., 2024; Liu et al., 2023). In contrast, *Labrys* and *Caulobacter* were enriched in cultures but were rare in sediments. While *Labrys* has no established association with Mn transformation, *Caulobacter* is a well-documented Mn oxidizer (Gounot, 1994; Kurt, 2019).

In contrast to lithotrophic cultures, communities enriched in cultures of organotrophic Mn oxidizers were highly variable and showed limited resemblance to sediment communities (Supplementary Figures S6C,D). 16S rRNA gene sequencing revealed distinct community shifts between July and October (Figures 7C,D, Supplementary Table S5). July cultures were dominated by the Mn reducers Trichococcus (Wang et al., 2018) and Clostridium (Lovley, 1991; Tebo et al., 2005), the latter also abundant in native sediments. October enrichments varied more and were dominated by Bacillus and Arenimonas, both of which were already abundant in the original sediment. Bacillus is a metabolically versatile genus capable of both Mn oxidation and reduction (Gounot, 1994; Kurt, 2019; Zakharova et al., 2010), while Arenimonas is known to perform Mn oxidation (Liu J. et al., 2018; Liu W. et al., 2018). Pseudomonas, capable of Mn transformation (Cai et al., 2023; Gounot, 1994; Lovley, 1991), became prominent in enrichments despite being initially low in sediments.

Communities enriched in cultures of Mn reducers formed distinct clusters, clearly separated from native sediment communities (Supplementary Figures S6E,F). Cultures were also grouped by inoculum origin, with nearly complete separation between cultures with sediment from buoys A and E in October. Community composition varied by sampling date and location (Figures 7E,F, Supplementary Table S5). In July, Rhodoferax dominated enrichments with sediment from buoy A, followed by Methanosarcina as the second most abundant genus. Bacillus appeared in deeper layers. In several cultures with sediment from buoys E and H, Aeromonas and Anaeromyxobacter were dominant, while Geothrix was the prevailing genus in one culture with sediment from buoy H. While Bacillus and Anaeromyxobacter were common in sediments, other dominant taxa were less abundant. Rhodoferax, Methanosarcina, Anaeromyxobacter, and Geothrix are all known Mn reducers (Chen et al., 2023; Coates et al., 1999; Finneran et al., 2003; Liu et al., 2023; Lovley et al., 1993), while Bacillus has the capacity for both Mn oxidation and reduction (Gounot, 1994; Kurt, 2019; Zakharova et al., 2010). Aeromonas, in contrast, is typically associated with Mn oxidation (Ehrlich and Newman, 2008; Shoiful et al., 2020; Zhang et al., 2019). In October, Bacillus again dominated enrichment cultures with sediment from buoy A and original sediments, while Rhodoferax appeared in several buoy E enrichments but remained rare in the original sediments.

Key metabolisms and the most representative genera identified by FAPROTAX and our own literature research are presented in more detail in Supplementary Figure S7, Supplementary Tables S6, S7.

4 Discussion

4.1 Redox-controlled Mn and Fe release from the sediment to the water column

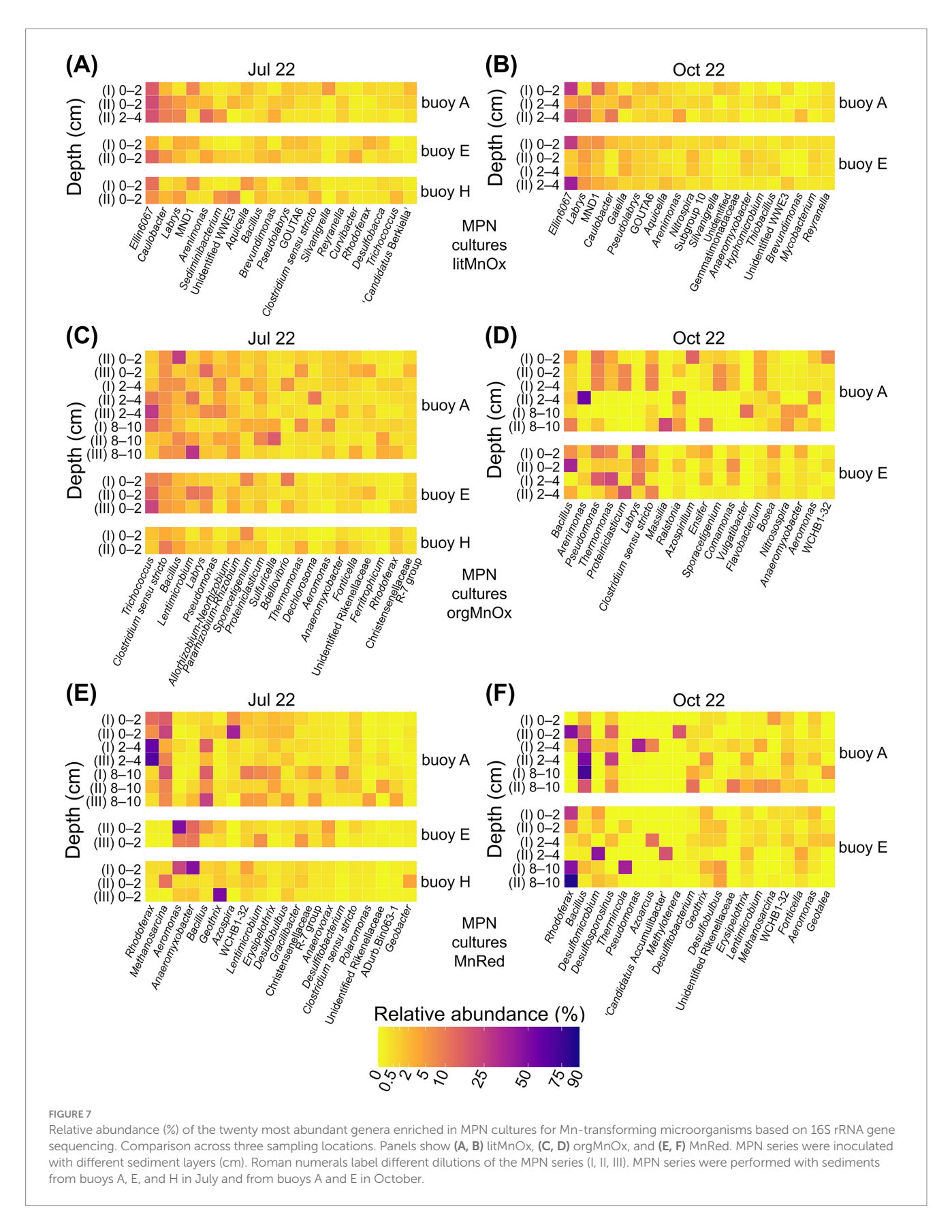
In the Wahnbach Reservoir, thermal stratification in summer and autumn (Supplementary Figure S1) leads to O_2 depletion, with concentrations dropping from ~300 μ M to 68 μ M at buoy A and to near-anoxic levels (3 μ M) at buoy E. Consumption of O_2 most likely

occurred through aerobically respiring organisms, including prokaryotes that use DOC as an electron donor. However, a concomitant decrease of DOC was not observed in bottom waters. In contrast, a slight increase was observed. Natural organic matter, including the dissolved organic matter (DOM) of freshwaters, consists of a huge diversity of organic molecules (Hertkorn et al., 2008) and varies considerably respective composition and reactivity (Dadi et al., 2017; Herzsprung et al., 2012, 2023). DOM adsorbs to mineral phases specifically to Fe (oxyhydr)oxides and to lesser extent to Mn (oxyhydr) oxides (Chorover and Amistadi, 2001; Ma et al., 2020) and may be released by reductive dissolution under anoxic conditions (Dadi et al., 2016, 2017).

Low-oxygen conditions promote Mn release from sediments via microbially mediated Mn oxide reduction (Herschel, 1995; Willmitzer et al., 2015). Dissolved Mn²⁺ is the dominant form in hypolimnetic waters (Godwin et al., 2020; Kamyshny et al., 2025; LaRowe et al., 2021), consistent with findings in water samples at buoy A, where acid-soluble Mn reached 83% Mn²⁺. Reservoir Mn levels vary regionally, with Wahnbach Reservoir values aligning with some studies (LaRowe et al., 2021; WHO, 2021). In many reservoirs, Mn(II) is released from sediments earlier and under less reducing conditions than Fe(II), leading to elevated dissolved Mn concentrations during the onset of stagnation. With prolonged stagnation, however, more reducing conditions favor Fe(III) reduction, and dissolved Fe(II) often surpasses Mn(II) concentrations (Giles et al., 2016; Krueger et al., 2020; Wendt-Potthoff et al., 2014). In addition to sedimentary release, surface runoff and inflow can also represent a relevant source of Fe and Mn input to the water column and should not be neglected in the overall mass balance (Li et al., 2019; Munger et al., 2019). Fe levels in the water column of the Wahnbach Reservoir did not exceed Mn content at any time. Due to its lower redox potential, Fe was released only under stronger reducing conditions (Durn et al., 2001; Lovley, 1995; Lovley and Phillips, 1988), here in sediments at buoy E reaching up to $5.9 \mu M$.

If all Mn(II) present in bottom waters at buoys A and E (9.4 and 24 µM, respectively) were oxidized to Mn(IV), this process could theoretically consume up to 4.7 and 12 μM O₂. Accordingly, complete reoxidation of Fe(II) to Fe(III) would require an additional 1.5 μM O₂ in waters above the sediment at buoy E. These values illustrate the potential contribution of inorganic electron donors (Mn2+, Fe2+) to aerobic respiration, in comparison with the generally much larger O2 demand driven by the oxidation of organic carbon (in bottom waters up to 138 μM at buoy A and 161 μM at buoy E). In the natural environment, these processes are highly dynamic with varying turnover rates as Mn(II) and Fe(II) are replenished from the sediment by reduction processes, while O₂ diffuses downward from overlying oxic water layers. Additionally, the processes by which reoxidation occurs may differ (abiotic vs. biotic). However, O2 is the strongest and most common oxidant available; its consumption in natural waters may be shared between abiotic and biotic processes and between chemoorganotrophic (organic C oxidation) and chemolithotrophic processes (oxidation of reduced Mn, Fe, or NH₄⁺). As indicated here, although inorganic electron donors can contribute to O2 consumption, their relative share is generally minor compared with that of organic matter oxidation.

Furthermore, low concentrations of NO_3^- in bottom waters (Supplementary Figure S1N) suggest denitrification. Such depletion is typical in deeper waters above the sediment, where denitrification often represents the dominant pathway of NO_3^- loss, reducing



 NO_3^- to N_2 and thereby limiting its accumulation in bottom waters. Together, lower NO_3^- values and Mn/Fe enrichment at the sediment-water interface under low O_2 conditions and high organic carbon

contents point to anaerobic processes such as denitrification and Mn(IV)/Fe(III) reduction (Forsberg, 1989; Hamilton-Taylor and Davison, 1995; Jiang Y. et al., 2024; Zhang D. et al., 2022).

4.2 Mn and Fe dynamics in reservoir sediments

Sediments in lakes and reservoirs act as sinks or sources for nutrients and redox-sensitive metals, depending on redox conditions at the sediment-water interface (Forsberg, 1989; Krueger et al., 2020). In Wahnbach Reservoir sediments (Figure 3), Mn reached up to 28 mM (15.6 g kg⁻¹) in surface layers at the deepest sampling location (buoy A), likely due to Mn focusing (Scholtysik et al., 2020; Scholtysik et al., 2022). These levels exceed typical freshwater sediment Mn concentrations of 0-7 g kg⁻¹ (von Gunten et al., 1997; Krueger et al., 2020; LaRowe et al., 2021; Madison et al., 2013). Usually, Fe exceeds Mn in sediments (Durn et al., 2001; Patrick and Henderson, 1981); however, here, Mn was comparably high. The extraction methods targeted Mn and Fe (oxyhydr)oxides (Durn et al., 2001; Schwertmann and Taylor, 1989), with dithionite and oxalate isolating poorly and well-crystallized Mn oxides, such as manganite, bixbyite, and hausmannite, though oxalate extraction is generally less efficient (Canfield et al., 1993; Durn et al., 2001; Lenstra et al., 2021). For Fe, dithionite extracts secondary oxides while oxalate targets amorphous and poorly crystalline forms (Canfield et al., 1993; Durn et al., 2001; Lenstra et al., 2021). Unexpectedly, oxalate extracts contained more and Fe than dithionite extracts Supplementary Figures S3, S4). It also has to be noted that in our study, extracts also included Mn(II) and Fe(II) forms such as carbonates, acid volatile sulfides, and dissolved Mn2+/Fe2+ (Canfield et al., 1993; Poulton and Canfield, 2005).

Redox potentials (Figure 2) suggest that Mn in sediments predominantly exists as Mn(IV) oxides, since Mn(IV) reduction occurs at potentials below +300 to +200 mV (Gotoh and Patrick, 1972), while Fe(III) reduction requires more reducing conditions below +100 mV to -47 mV (Durn et al., 2001; Patrick and Henderson, 1981). However, depending on the mineral phases present, the redox potential ranges for Fe and Mn minerals, leading to zones where Mn(IV) and Fe(III) reduction and also other anaerobic respiration processes can occur (Fiskal et al., 2019; Liu J. et al., 2022; Lovley, 1991; Lovley et al., 2004). Comparisons of redox potential profiles in the sediment between sampling locations suggest localized heterogeneity, whereas temporal differences between sampling dates are likely linked to seasonal biogeochemical changes. Organic matter present in the sediment of the Wahnbach Reservoir most likely served as electron donor for the anaerobic respiration processes.

Pore water concentrations of dissolved Mn^{2+} and Fe^{2+} (Figures 4B,C) in sediments at buoy A were generally low and made up only a small fraction of total Mn and Fe extracted by dithionite or oxalate. In September, concentrations of dissolved Mn and Fe were higher in deeper layers, with Mn^{2+} exceeding Fe^{2+} , suggesting Mn(IV) and Fe(III) reduction to occur under reducing conditions, probably fueled by organic carbon degradation. The resulting Mn^{2+} and Fe^{2+} diffuse upward, where they may be reoxidized and redeposited, contributing to metal focusing. The biotically oxidation of Mn^{2+} can be very fast, so Mn^{2+} does not accumulate (Morgan, 2005). Mn^{2+} pore water levels in Wahnbach Reservoir reached up to 276 μ M, placing them at the higher end of values reported for freshwater systems (LaRowe et al., 2021).

The NH₄⁺ profile (Figure 4G) in the pore water showed higher concentrations of NH₄⁺ at greater depths. Degradation of organic matter and concomitant ammonification may be a source of NH₄⁺. It

indicates a consumption of ammonification in the surface sediment layer and/or overlying water. At the sediment surface, the observed decrease in NH₄⁺ is a result of nitrification, while the resulting NO₃⁻ is subsequently consumed through denitrification, and a smaller fraction of NO₃⁻ is likely reduced to NH₄⁺ via nitrate ammonification (Cojean et al., 2020). Therefore, low concentrations of NO₃⁻ (Figure 4F) were observed in the pore water. The process of nitrification can occur even at low O2 concentrations (Stenstrom and Poduska, 1980), with Mn oxides serving as electron acceptors, particularly in the upper sediment layers (Hulth et al., 1999). Additionally, in deeper sediment layers, SO_4^{2-} depletion (Figure 4D) indicates SO₄²-reduction. In the Wahnbach Reservoir, pH slightly decreased below 7 at the sediment-water interface, reaching lower values than in the overlying water column and the deeper sediment layers. This decrease is likely caused by the reoxidation of reduced inorganic compounds, including sulfide (reflected in elevated SO₄²⁻ concentrations at the sediment surface), Fe(II), and Mn(II) compounds. With depth, pH gradually increases, reflecting ongoing reductive processes in the sediments (Silburn et al., 2017).

Sediment and pore water profiles reflect a typical redox zonation in the Wahnbach Reservoir: denitrification in the sediment-water interface, as well as nitrification in surface sediments, followed by Mn(IV), Fe(III), and $SO_4^{\,2^-}$ reduction with increasing depth (Canfield and Thamdrup, 2009). Estimated potential electron acceptor concentrations are: (i) Fe(III) up to 74 mM (assuming that most of the extracted Fe is accounted by Fe oxides), (ii) Mn(IV) up to 28 mM (assuming that most of the extracted Mn is accounted by Mn oxides), (iii) $SO_4^{\,2^-}$ up to 438 μ M, and (iv) $NO_3^{\,-}$ < 1 μ M, whereby the high NH_4^+ concentrations (increasing to 127 μ M) indicate production from organic matter degradation, with $NO_3^{\,-}$ appearing only transiently as an intermediate and being rapidly consumed through denitrification. Organic carbon will be one of the most important electron donors in this context.

4.3 Key prokaryotic players driving redox processes in sediments

The dominant prokaryotic classes in Wahnbach Reservoir sediments (Supplementary Figure S5) were consistent across sampling locations and dates, typical of freshwater lakes and sediments (Huang et al., 2017; Newton et al., 2011; Song et al., 2024; Wu et al., 2017; Zemskaya et al., 2021; Zhang et al., 2019). The distribution of the community likely reflects general redox zonation and/or organic carbon availability. More detailed insights into metabolic processes were obtained from 16S rRNA gene sequencing results at the genus level, which reflected redox changes and were supported by physicochemical data, consistent with typical patterns in freshwater sediments (Canfield and Thamdrup, 2009).

Although Mn and Fe concentrations were high in sediments, especially at buoy A, and elevated Mn²⁺ and Fe²⁺ levels in pore water suggested Mn(IV) and Fe(III) reduction, FAPROTAX detected few sequences linked to Fe-transforming prokaryotes and almost none for Mn-transformers (Figure 6). This discrepancy highlights a common limitation of predictive functional tools, which rely on curated reference databases and cultured representatives (Djemiel et al., 2022; Sansupa et al., 2021). Many genera with experimentally confirmed Mn-transforming ability, such as *Clostridium*, *Bacillus*, or

Anaeromyxobacter, are not explicitly annotated in FAPROTAX, which may result in their underrepresentation. Literature research revealed that Mn-transforming taxa were far more widespread than suggested by the automated annotation.

Despite their apparently modest relative abundances, Mn- and Fe-transforming prokaryotes can play disproportionally large roles in sediment redox dynamics (Canfield et al., 2005; Lovley, 2006). Both metals often act as electron acceptors in anoxic environments, for example, facilitating the oxidation of organic carbon, and serve as redox partners in the reduction of $\mathrm{NO_3}^-$ and $\mathrm{SO_4}^{2-}$ or during methanogenesis. Importantly, many Mn-associated prokaryotes in sediments of the Wahnbach Reservoir are not restricted to metal cycling but are metabolically versatile, participating simultaneously in other elemental cycles. Such multiple metabolic roles suggest that Mn cycling in freshwater sediments cannot be understood in isolation but must be considered in a broader Mn-Fe-S-N-C network.

Depth-resolved patterns reflect classical redox zonation in sediments, where Mn and Fe reduction typically occur beneath the zone of declining O₂ concentrations and low NO₃⁻ availability, followed by SO₄²⁻ reduction and methanogenesis (Berg et al., 1998; Canfield and Thamdrup, 2009; Fiskal et al., 2019). Observed substantial Mn-reducing genera alongside only moderate abundances of SO₄²⁻ reducers suggests that Mn and Fe play a stronger role in controlling anaerobic organic matter turnover in sediments of the Wahnbach Reservoir compared to SO₄²⁻. This is consistent with the relatively high organic matter content (~5-10%), which supports anaerobic degradation and methane production. While no visible methane release was observed, Mn cycling may suppress methanogenesis, as suggested in previous studies (Ma et al., 2008). Organisms associated with nitrification were relatively abundant, indicating that NH₄⁺ produced in deeper layers is actively metabolized in surface sediment. Although organisms linked to NO₃⁻ respiration were less abundant, this process nonetheless plays an important role in shaping sediment biogeochemistry, as discussed above. The ecological relevance of Mn cycling has broader implications (Wang et al., 2022). Freshwater reservoirs often rely on the cycling of Mn and also Fe to regulate carbon turnover and CH₄ production (Leu et al., 2020; Ma et al., 2008; Su et al., 2020). In marine sediments, SO₄²⁻ reducers often dominate and suppress methanogenesis (Su et al., 2020), rather than other electron acceptors, such as NO₃-, Mn, and Fe compounds.

4.4 Mn-transforming prokaryotes enriched in MPN cultures

Coloration and discoloration of MPN cultures, especially at higher dilutions, indicated biotic Mn oxidation and reduction. Prokaryotes abundant at higher dilutions likely thrived under selective conditions and may contribute to Mn cycling in Wahnbach Reservoir sediments, as observed for Mn reducer cultures. No clear growth was observed in lithotrophic Mn oxidizer cultures, whereas organotrophic Mn oxidizers peaked at the deepest sampling location, where Mn and organic matter were abundant (Supplementary Table S4). Mn reducers were consistently detected at all sampling locations, with MPN around 10^3 – 10^4 mL⁻¹, comparable to values in the Rappbode Reservoir, Germany (Wendt-Potthoff et al., 2014).

In lithotrophic Mn oxidizer cultures, minimal Mn oxidation and Mn-dependent growth were observed, even at the lowest dilution. Thus, extracted DNA (Figures 7A,B, Supplementary Tables S5–S7) likely came from sediment organisms such as *Ellin6067*, possibly growing on sediment-derived substrates with little influence from Mn. Enriched organisms, such as *Caulobacter*, an aerobic chemoorganotroph (Abraham et al., 1999), likely utilized organic matter from the sediment (Gounot, 1994; Kurt, 2019). Although it appeared to have a limited impact in the original sediments, it derived an advantage for growth from enrichment cultures for Mn oxidizers. Overall, lithotrophic Mn oxidizers likely play a minor role in Mn cycling in the Wahnbach Reservoir.

In organotrophic Mn oxidizer cultures (Figures 7C,D, Supplementary Tables S5-S7), a diverse community was enriched, including known Mn-oxidizing and -reducing prokaryotes. Abundant and enriched Mn oxidizers, such as Arenimonas (Liu et al., 2018), might play a major role here, whereby Mn oxidizers such as Thermomonas (Li et al., 2024; Yang et al., 2014) were also enriched, which, due to their low abundance in the original sediment, are probably not of great importance for the Mn cycle in the Wahnbach Reservoir, but showed a high potential for active Mn oxidation. The same apply to the enriched Mn-transforming organisms Bacillus (Gounot, 1994; Kurt, 2019; Zakharova et al., 2010), already abundant in original sediments, and Pseudomonas (Gounot, 1994; Tebo et al., 2004; Zakharova et al., 2010), previously detected in low abundance. Their enrichment and associated medium discoloration suggest a role in Mn oxidation. The enrichment of genera that are already quite abundant in sediments demonstrates their relevance for active Mn cycling in the Wahnbach Reservoir. Surprisingly, the typical Mn reducers Trichococcus (Wang et al., 2018) and Clostridium (Lovley, 1991; Tebo et al., 2005) were observed. Clostridium, already abundant in sediments, likely persisted due to low dilution, while Trichococcus, a facultative anaerobe, may have thrived on available organic matter. The enriched community reflects adaptation to varied conditions.

In Mn reducer cultures (Figures 7E, F, Supplementary Tables S5–S7), various prokaryotes capable of Mn reduction or both Mn oxidation and reduction were enriched. Due to higher dilutions, these cultures were less influenced by the original sediment community and exhibited clear Mn(IV) reduction, as indicated by discoloration. Anaeromyxobacter, abundant in sediments, was enriched in cultures from buoys E and H, supporting its role in active Mn reduction (Liu et al., 2023; Liu et al., 2020; Wang et al., 2020), potentially coupled to anaerobic CH₄ oxidation in the original sediments. Rhodoferax, initially less abundant, was strongly enriched, benefiting from the organic-rich medium while reducing Mn(IV) and Fe(III) (Finneran et al., 2003; Kato and Ohkuma, 2021). Methanosarcina enrichment in cultures from buoy A, where it was already present, suggests involvement in anaerobic CH4 oxidation coupled to Mn reduction (Chen et al., 2023; Liu et al., 2020; Yu et al., 2022) in the Wahnbach Reservoir sediments. Azospira, initially rare, was enriched in upper layer cultures from buoy A, indicating Mn's relevance in NO₃respiration (Peng et al., 2016; Tong et al., 2023). Genera such as Desulfomicrobium, Desulfosporosinus, and Desulfitobacterium (Kim et al., 2012; Sharak Genthner and Devereux, 2015; Thevenieau et al., 2007; Villemur et al., 2006), previously less abundant, were also enriched, likely coupling organic oxidation with Mn(IV) reduction. These findings underscore the abundance and diversity of Mn-reducing microbes, their wide repertoire of utilizing and linking

different metabolic pathways, and the significance of Mn reduction in the Wahnbach Reservoir.

The enrichment of genera enriched in both cultures of Mn reducers and (organotrophic) Mn oxidizers, along with the presence of prokaryotes exhibiting various Mn-associated metabolisms in the sediment, highlighted the adaptability of the prokaryotic community in the Wahnbach Reservoir. Additionally, the enrichment of genera previously in low abundances in sediments suggests that under more reducing conditions, Mn reduction could increase, leading to greater Mn release into the water column of the Wahnbach Reservoir.

5 Conclusion

The metabolic pathways identified in this study reveal a complex and tightly interconnected biogeochemical network in the Wahnbach Reservoir, linking the cycling of Mn, Fe, N, S, and C (Cojean et al., 2020; Gounot, 1994; Hulth et al., 1999; Pimenov and Neretin, 2006; Su et al., 2020; Thamdrup et al., 2000; Wallenius et al., 2021). Key prokaryote-mediated processes shaping this network include: (i) Mn(IV) and Fe(III) reduction primarily in deeper sediment layers, with dissolved Mn(II) and Fe(II) largely retained and reoxidized in surface layers; (ii) probably ammonification in deeper layers coupled to nitrification and denitrification in upper layers and the sedimentwater interface, (iii) sulfate reduction occurring in deeper, anoxic zones; and (iv) potential methane production in the deeper sediments, counterbalanced by CH₄ oxidation in the surface sediments. These processes align with established redox stratification patterns commonly found in freshwater systems (Berg et al., 1998; Canfield and Thamdrup, 2009; Fiskal et al., 2019).

The presence of Mn in the water column reflects episodic shifts toward more reducing conditions, often during stratification or stimulated organic carbon production. In the Wahnbach Reservoir, sediment processes regulate which reduced compounds are released or retained. In particular, in-sediment reoxidation of reduced compounds appears to act as a critical barrier to the release of NH₄⁺, partially Fe(II), H₂S/HS⁻, and CH₄ into the overlying water. Simultaneously, the regeneration of Mn(IV), Fe(III), NO₃⁻, and SO₄²⁻, which act as alternative terminal electron acceptors, sustain redox cycling within the sediment. Importantly, NO₃⁻ and SO₄²⁻ can also be replenished in the absence of O2 and contribute significantly due to high turnover. Mn(IV) reduction emerges as a pivotal process, supported by the availability of Mn(IV) in sediments and the presence of prokaryotes capable of coupling its reduction with the oxidation of NH₄⁺, S compounds, organic matter, and CH₄ (Godwin et al., 2020; Gounot, 1994; Lovley, 1991; Wang et al., 2022).

Our results, therefore, extend the general consensus on redox zonation and metal accumulation by emphasizing the regulatory role of sediments as both sources and sinks. In contrast to much of the literature, where Mn and Fe are often discussed together, our data demonstrate that their roles and dynamics differ substantially. Although some microorganisms are capable of reducing both Mn and Fe, many are specialized, and their activities are further separated by the markedly different redox potentials required for Mn(IV) and Fe(III) reduction. Moreover, predictive tools such as FAPROTAX underestimate several taxa with confirmed Mn- or Fe-transforming capacities, leading to an underappreciation of their ecological relevance. In the Wahnbach Reservoir, Mn cycling in

particular emerges as disproportionately important: Mn transformation is a key pathway tightly linked to N, S, and C transformations (Wang et al., 2022). This coupling makes Mn a central node in controlling water column chemistry and, by extension, drinking water quality.

Redox dynamics are particularly important for drinking water management. Sustained reducing conditions can enhance the mobilization of Mn(II), necessitating additional treatment efforts. In the Wahnbach Reservoir, differences between sampling locations highlight the central role of local redox conditions, as overall O2 concentrations, or their absence, represent one of the most important predictors of Mn release and accumulation. Since input from surface runoff or atmospheric deposition can be largely ruled out here, Mn cycling is primarily governed by in-sediment processes. Mn reduction sets in rapidly once O2 levels decline, and the rates of biotic reduction depend on both the content and type of Mn minerals, the availability of electron donors (including organic carbon, NH₄⁺, and CH₄), and the ecophysiology of the microbial community. Equally important are reoxidation processes, which strongly affect the net accumulation of Mn in bottom waters; abiotic pathways, in particular, can play a key role (Ma et al., 2020). Thus, continuous monitoring of redox-sensitive parameters in the Wahnbach Reservoir is essential to assess the potential for Mn release, its dependency on local redox changes, and the underlying microbial and geochemical mechanisms driving Mn cycling. Understanding these interactions is key to anticipating and mitigating water quality challenges under changing environmental conditions.

Data availability statement

The datasets presented in this study are publicly available. This data can be found at: https://www.ncbi.nlm.nih.gov/sra, accession number PRJNA1263398.

Author contributions

LH: Writing – original draft, Project administration, Formal analysis, Software, Visualization, Methodology, Resources, Investigation, Validation, Conceptualization, Data curation, Writing – review & editing. SV: Visualization, Formal analysis, Investigation, Software, Writing – review & editing. GP: Writing – review & editing, Supervision, Data curation, Methodology, Resources, Funding acquisition, Conceptualization, Project administration, Validation. JM: Supervision, Conceptualization, Funding acquisition, Writing – review & editing, Resources, Project administration. WM: Supervision, Writing – review & editing, Funding acquisition, Conceptualization, Resources.

Funding

The author(s) declare that financial support was received for the research and/or publication of this article. This work was funded by the State of Rhineland-Palatinate, Germany, as part of a research initiative, and by the Wahnbach Reservoir Association (Wahnbachtalsperrenverband – WTV), Germany, as part of a research and development (R&D) project.

Acknowledgments

The authors acknowledge Annika Fiskal and Jens Hahn (Federal Institute for Hydrology, Koblenz) and Katrin Wendt-Potthoff (Helmholtz-Centre for Environmental Research, Magdeburg) for sharing their expertise and knowledge on sediment sampling, physicochemical measurements, and cultivation techniques. Gratitude is extended to Dorothée Karger and Gerhard Dawen (Biological-Ecological Station, Bettenfeld) for their assistance with the sediment corer. The authors thank Kerstin Hoffmann, Ulli Bange, and Brigitte Mann (University of Koblenz), as well as Matthias Gerhardt (Wahnbach Reservoir Association, Wahnbachtalsperrenverband – WTV, Siegburg), for their technical support. Thanks are due to Michael Götten and Meike Köster for their technical expertise, and to Simon Nickel and Kevin Jäger for additional assistance. Appreciation is owed to Yvonne Werle and Ricarda Diedrichs for their writing advice.

Conflict of interest

The authors declare that the research was conducted in the absence of any commercial or financial relationships that could be construed as a potential conflict of interest.

References

Abraham, W. R., Strömpl, C., Meyer, H., Lindholst, S., Moore, E. R. B., Christ, R., et al. (1999). Phylogeny and polyphasic taxonomy of *Caulobacter* species. Proposal of *Maricaulis* gen. Nov. with *Maricaulis maris* (Poindexter) comb. nov. as the type species, and emended description of the genera *Brevundimonas* and *Caulobacter*. *Int. J. Syst. Evol. Microbiol.* 49, 1053–1073. doi: 10.1099/00207713-49-3-1053

Berg, P., Risgaard-Petersen, N., and Rysgaard, S. (1998). Interpretation of measured concentration profiles in sediment pore water. *Limnol. Oceanogr.* 43, 1500–1510. doi: 10.4319/lo.1998.43.7.1500

Bokulich, N. A., Kaehler, B. D., Rideout, J. R., Dillon, M., Bolyen, E., Knight, R., et al. (2018). Optimizing taxonomic classification of marker-gene amplicon sequences with QIIME 2's q2-feature-classifier plugin. *Microbiome* 6:90. doi: 10.1186/s40168-018-0470-z

Bolyen, E., Rideout, J. R., Dillon, M. R., Bokulich, N. A., Abnet, C. C., Al-Ghalith, G. A., et al. (2019). Reproducible, interactive, scalable and extensible microbiome data science using QIIME 2. *Nat. Biotechnol.* 37, 852–857. doi: 10.1038/s41587-019-0209-9

Boogerd, F. C., and de Vrind, J. P. (1987). Manganese oxidation by *Leptothrix discophora*. *J. Bacteriol.* 169, 489–494. doi: 10.1128/jb.169.2.489-494.1987

Bryant, L. D., Little, J. C., and Bürgmann, H. (2012). Response of sediment microbial community structure in a freshwater reservoir to manipulations in oxygen availability. *FEMS Microbiol. Ecol.* 80, 248–263. doi: 10.1111/j.1574-6941.2011.01290.x

Cai, Y., Yang, K., Qiu, C., Bi, Y., Tian, B., and Bi, X. (2023). A review of manganese-oxidizing bacteria (MnOB): applications, future concerns, and challenges. *Int. J. Environ. Res. Public Health* 20:1272. doi: 10.3390/ijerph20021272

Callahan, B. J., McMurdie, P. J., Rosen, M. J., Han, A. W., Johnson, A. J. A., and Holmes, S. P. (2016). Dada2: high-resolution sample inference from Illumina amplicon data. *Nat. Methods* 13, 581–583. doi: 10.1038/nmeth.3869

Canfield, D. E., Kristensen, E., and Thamdrup, B. (2005). The iron and manganese cycles. *Adv. Mar. Biol.* 48, 269–312. doi: 10.1016/S0065-2881(05)48008-6

Canfield, D. E., and Thamdrup, B. (2009). Towards a consistent classification scheme for geochemical environments, or, why we wish the term 'suboxic' would go away. *Geobiology* 7, 385–392. doi: 10.1111/j.1472-4669.2009.00214.x

Canfield, D. E., Thamdrup, B., and Hansen, J. W. (1993). The anaerobic degradation of organic matter in Danish coastal sediments: iron reduction, manganese reduction, and sulfate reduction. *Geochim. Cosmochim. Acta* 57, 3867–3883. doi: 10.1016/0016-7037(93)90340-3

Carmichael, S. K., and Bräuer, S. L. (2015). "Microbial diversity and manganese cycling: a review of manganese-oxidizing microbial cave communities" in Microbial life

Generative AI statement

The authors declare that no Gen AI was used in the creation of this manuscript.

Any alternative text (alt text) provided alongside figures in this article has been generated by Frontiers with the support of artificial intelligence and reasonable efforts have been made to ensure accuracy, including review by the authors wherever possible. If you identify any issues, please contact us.

Publisher's note

All claims expressed in this article are solely those of the authors and do not necessarily represent those of their affiliated organizations, or those of the publisher, the editors and the reviewers. Any product that may be evaluated in this article, or claim that may be made by its manufacturer, is not guaranteed or endorsed by the publisher.

Supplementary material

The Supplementary material for this article can be found online at: https://www.frontiersin.org/articles/10.3389/fmicb.2025.1671749/full#supplementary-material

of cave systems. Life in extreme environments. ed. A. S. Engel (Boston, MA: De Gruvter), 137–160.

Chen, Q., Wang, N., Huang, D., Yuan, T., Wu, H., and Xu, Q. (2023). Enhancement of methane production from anaerobic digestion using different manganese species. *Biomass Convers. Biorefinery* 13, 9783–9793. doi: 10.1007/s13399-021-01839-6

Cheng, Q., Nengzi, L., Bao, L., Huang, Y., Liu, S., Cheng, X., et al. (2017). Distribution and genetic diversity of microbial populations in the pilot-scale biofilter for simultaneous removal of ammonia, iron and manganese from real groundwater. *Chemosphere* 182, 450–457. doi: 10.1016/j.chemosphere.2017.05.075

Chorover, J., and Amistadi, M. K. (2001). Reaction of forest floor organic matter at goethite, birnessite and smectite surfaces. *Geochim. Cosmochim. Acta* 65, 95–109. doi: 10.1016/S0016-7037(00)00511-1

Coates, J. D., Ellis, D. J., Gaw, C. V., and Lovley, D. R. (1999). *Geothrix fermentans* gen. Nov., sp. nov., a novel fe(III)-reducing bacterium from a hydrocarbon-contaminated aquifer. *Int. J. Syst. Bacteriol.* 49, 1615–1622. doi: 10.1099/00207713-49-4-1615

Cojean, A. N. Y., Lehmann, M. F., Robertson, E. K., Thamdrup, B., and Zopfi, J. (2020). Controls of H_2S , Fe^{2+} , and Mn^{2+} on microbial NO^{3-} -reducing processes in sediments of an eutrophic lake. *Front. Microbiol.* 11:1158. doi: 10.3389/fmicb.2020.01158

Corstjens, P. L. A. M., de Vrind, J. P. M., Goosen, T., and Jong, E. W. d. V. (1997). Identification and molecular analysis of the *Leptothrix discophora* SS-1 *mofA* gene, a gene putatively encoding a manganese-oxidizing protein with copper domains. *Geomicrobiol. J.* 14, 91–108. doi: 10.1080/01490459709378037

Dadi, T., Friese, K., Wendt-Potthoff, K., and Koschorreck, M. (2016). Benthic dissolved organic carbon fluxes in a drinking water reservoir. *Limnol. Oceanogr.* 61, 445–459. doi: 10.1002/lno.10224

Dadi, T., Harir, M., Hertkorn, N., Koschorreck, M., Schmitt-Kopplin, P., and Herzsprung, P. (2017). Redox conditions affect dissolved organic carbon quality in stratified freshwaters. *Environ. Sci. Technol.* 51, 13705–13713. doi: 10.1021/acs.est.7b04194

Davison, W. (1993). Iron and manganese in lakes. *Earth-Sci. Rev.* 34, 119–163. doi: 10.1016/0012-8252(93)90029-7

Delpla, I., Jung, A.-V., Baures, E., Clement, M., and Thomas, O. (2009). Impacts of climate change on surface water quality in relation to drinking water production. *Environ. Int.* 35, 1225–1233. doi: 10.1016/j.envint.2009.07.001

Diem, D., and Stumm, W. (1984). Is dissolved Mn^{2+} being oxidized by O_2 in absence of Mn-bacteria or surface catalysts? *Geochim. Cosmochim. Acta* 48, 1571–1573. doi: 10.1016/0016-7037(84)90413-7

- Djemiel, C., Maron, P.-A., Terrat, S., Dequiedt, S., Cottin, A., and Ranjard, L. (2022). Inferring microbiota functions from taxonomic genes: a review. *Gigascience* 11:giab090. doi: 10.1093/gigascience/giab090
- Durn, G., Pavelić, D., and Čović, M. (2001). Distribution of iron and manganese in Terra Rossa from Istria and its genetic implications. *Geol. Croat.* 54, 27–36. doi: 10.4154/GC.2001.03
- Dürre, P. (2015). Clostridia. eLS 1–11. Wiley (Hoboken, NJ). doi: 10.1002/9780470015902.a0020370.pub2
- Edgar, R. C. (2004). MUSCLE: multiple sequence alignment with high accuracy and high throughput. *Nucleic Acids Res.* 32, 1792–1797. doi: 10.1093/nar/gkh340
- Edgar, R. C. (2013). UPARSE: highly accurate OTU sequences from microbial amplicon reads. *Nat. Methods* 10, 996–998. doi: 10.1038/nmeth.2604
- Ehrlich, H. L., and Newman, D. K. (2008). Geomicrobiology. Boca Raton, FL: CRC Press
- Emerson, D. (2000). "Microbial oxidation of fe (II) and Mn (II) at circumneutral pH" in Environmental microbe-metal interactions. ed. D. R. Lovley (Washington, DC: ASM Press), 31–52.
- European Parliament and Council of the European Union (2020). Directive (EU) 2020/2184 of the European Parliament and of the council of 16 December 2020 on the quality of water intended for human consumption (recast) (text with EEA relevance). Off. J. Eur. Union. Available online at: https://eur-lex.europa.eu/eli/dir/2020/2184/oj (Accessed July 16, 2025).
- Finneran, K. T., Johnsen, C. V., and Lovley, D. R. (2003). *Rhodoferax ferrireducens* sp. nov., a psychrotolerant, facultatively anaerobic bacterium that oxidizes acetate with the reduction of fe (III). *Int. J. Syst. Evol. Microbiol.* 53, 669–673. doi: 10.1099/ijs.0.02298-0
- Firoozi, F., Roozbahani, A., and Massah Bavani, A. R. (2020). Developing a framework for assessment of climate change impact on thermal stratification of dam reservoirs. *Int. J. Environ. Sci. Technol.* 17, 2295–2310. doi: 10.1007/s13762-019-02544-8
- Fiskal, A., Deng, L., Michel, A., Eickenbusch, P., Han, X., Lagostina, L., et al. (2019). Effects of eutrophication on sedimentary organic carbon cycling in five temperate lakes. *Biogeosciences* 16, 3725–3746. doi: 10.5194/bg-16-3725-2019
- Forsberg, C. (1989). Importance of sediments in understanding nutrient cyclings in lakes. Hydrobiologia 176-177, 263–277. doi: 10.1007/BF00026561
- Francis, C. A., Casciotti, K. L., and Tebo, B. M. (2002). Localization of Mn(II)-oxidizing activity and the putative multicopper oxidase, MnxG, to the exosporium of the marine *bacillus* sp. strain SG-1. *Arch. Microbiol.* 178, 450–456. doi: 10.1007/s00203-002-0472-9
- Francis, A. J., and Dodge, C. J. (1991). Dissolution of ferrites by Clostridium sp. Geomicrobiol J. 9, 27–40. doi: 10.1080/01490459109385983
- Friedman, A., Boselli, E., Ogneva-Himmelberger, Y., Heiger-Bernays, W., Brochu, P., Burgess, M., et al. (2024). Manganese in residential drinking water from a community-initiated case study in Massachusetts. *J. Expo. Sci. Environ. Epidemiol.* 34, 58–67. doi: 10.1038/s41370-023-00563-9
- Frisbie, S. H., Mitchell, E. J., Dustin, H., Maynard, D. M., and Sarkar, B. (2012). World Health Organization discontinues its drinking-water guideline for manganese. *Environ. Health Perspect.* 120, 775–778. doi: 10.1289/ehp.1104693
- Geist, J., and Auerswald, K. (2007). Physicochemical stream bed characteristics and recruitment of the freshwater pearl mussel (*Margaritifera margaritifera*). *Freshw. Biol.* 52, 2299–2316. doi: 10.1111/j.1365-2427.2007.01812.x
- Giles, C. D., Isles, P. D. F., Manley, T., Xu, Y., Druschel, G. K., and Schroth, A. W. (2016). The mobility of phosphorus, iron, and manganese through the sediment-water continuum of a shallow eutrophic freshwater lake under stratified and mixed water-column conditions. *Biogeochemistry* 127, 15–34. doi: 10.1007/s10533-015-0144-x
- Godwin, C. M., Zehnpfennig, J. R., and Learman, D. R. (2020). Biotic and abiotic mechanisms of manganese (II) oxidation in Lake Erie. *Front. Environ. Sci.* 8:57. doi: 10.3389/fenvs.2020.00057
- Gotoh, S., and Patrick, W. H. (1972). Transformation of manganese in a waterlogged soil as affected by redox potential and pH. *Soil Sci. Soc. Am. J.* 36, 738–742. doi: 10.2136/sssaj1972.03615995003600050018x
- Gotore, O., Watanabe, M., Okano, K., Miyata, N., Katayama, T., Yasutaka, T., et al. (2025). Effects of batch and continuous-flow operation on biotreatment of Mn(II)-containing mine drainage. *J. Environ. Sci.* 152, 401–415. doi: 10.1016/j.jes.2024.05.038
- Gounot, A. M. (1994). Microbial oxidation and reduction of manganese: consequences in groundwater and applications. *FEMS Microbiol. Rev.* 14, 339–349. doi: 10.1111/j.1574-6976.1994.tb00108.x
- Grady, E. N., MacDonald, J., Liu, L., Richman, A., and Yuan, Z.-C. (2016). Current knowledge and perspectives of *Paenibacillus*: a review. *Microb. Cell Factories* 15:203. doi: 10.1186/s12934-016-0603-7
- Hamilton-Taylor, J., and Davison, W. (1995). "Redox-driven cycling of trace elements in lakes" in Physics and chemistry of lakes. eds. A. Lerman, D. M. Imboden and J. R. Gat (Berlin: Springer), 217–263.
- Herschel, A. (1995). Auflösung und Ausfällung von Mangan in stehenden Oberflächengewässern. Dresden: Technische Universität Dresden.

- Hertkorn, N., Frommberger, M., Witt, M., Koch, B. P., Schmitt-Kopplin, P., and Perdue, E. M. (2008). Natural organic matter and the event horizon of mass spectrometry. *Anal. Chem.* 80, 8908–8919. doi: 10.1021/ac800464g
- Herzsprung, P., von Tümpling, W., Hertkorn, N., Harir, M., Büttner, O., Bravidor, J., et al. (2012). Variations of DOM quality in inflows of a drinking water reservoir: linking of van Krevelen diagrams with EEMF spectra by rank correlation. *Environ. Sci. Technol.* 46, 5511–5518. doi: 10.1021/es300345c
- Herzsprung, P., Kamjunke, N., Wilske, C., Friese, K., Boehrer, B., Rinke, K., et al. (2023). Data evaluation strategy for identification of key molecular formulas in dissolved organic matter as proxies for biogeochemical reactivity based on abundance differences from ultrahigh resolution mass spectrometry. *Water Res.* 232:119672. doi: 10.1016/j.watres.2023.119672
- $Holmer, M., and Storkholm, P. (2001). Sulphate reduction and Sulphur cycling in lake sediments: a review. {\it Freshw. Biol.} 46, 431–451. doi: 10.1046/j.1365-2427.2001.00687.x$
- Horsburgh, M. J., Wharton, S. J., Karavolos, M., and Foster, S. J. (2002). Manganese: elemental defence for a life with oxygen. *Trends Microbiol.* 10, 496–501. doi: 10.1016/S0966-842X(02)02462-9
- Huang, W., Chen, X., Jiang, X., and Zheng, B. (2017). Characterization of sediment bacterial communities in plain lakes with different trophic statuses. *Microbiology* 6:e00503. doi: 10.1002/mbo3.503
- Hulth, S., Aller, R. C., and Gilbert, F. (1999). Coupled anoxic nitrification/manganese reduction in marine sediments. *Geochim. Cosmochim. Acta* 63, 49–66. doi: 10.1016/S0016-7037(98)00285-3
- Ji, Y., Angel, R., Klose, M., Claus, P., Marotta, H., Pinho, L., et al. (2016). Structure and function of methanogenic microbial communities in sediments of Amazonian lakes with different water types. *Environ. Microbiol.* 18, 5082–5100. doi: 10.1111/1462-2920.13491
- Jiang, Z., Huang, X., Wang, S., Xiong, J., Xie, C., and Chen, Y. (2024). Divalent manganese stimulates the removal of nitrate by anaerobic sludge. *RSC Adv.* 14, 2447–2452. doi: 10.1039/D3RA07088C
- Jiang, Y., Xie, Z., Ding, M., Zhang, H., Huang, G., Cao, Y., et al. (2024). Sediment nitrate dissimilatory reduction processes in the river-Lake ecotone of Poyang lake, China: mechanisms and environmental implications. *J. Soils Sediments* 24, 3515–3529. doi: 10.1007/s11368-024-03890-y
- Kamyshny, A., Klein, R., Eckert, W., and Avetisyan, K. (2025). Influence of environmental settings, including vegetation, on speciation of the redox-sensitive elements in the sediments of monomictic Lake Kinneret. *Limnology* 26, 1–18. doi: 10.1007/s10201-024-00756-7
- Kanso, S., Greene, A. C., and Patel, B. K. C. (2002). *Bacillus subterraneus* sp. nov., an iron- and manganese-reducing bacterium from a deep subsurface Australian thermal aquifer. *Int. J. Syst. Evol. Microbiol.* 52, 869–874. doi: 10.1099/00207713-52-3-869
- Kato, S., and Ohkuma, M. (2021). A single bacterium capable of oxidation and reduction of iron at circumneutral pH. *Microbiol. Spectr.* 9:e0016121. doi: 10.1128/spectrum.00161-21
- Kim, S.-H., Harzman, C., Davis, J. K., Hutcheson, R., Broderick, J. B., Marsh, T. L., et al. (2012). Genome sequence of *Desulfitobacterium hafriiense* DCB-2, a gram-positive anaerobe capable of dehalogenation and metal reduction. *BMC Microbiol.* 12:21. doi: 10.1186/1471-2180-12-21
- Krueger, K. M., Vavrus, C. E., Lofton, M. E., McClure, R. P., Gantzer, P., Carey, C. C., et al. (2020). Iron and manganese fluxes across the sediment-water interface in a drinking water reservoir. *Water Res.* 182:116003. doi: 10.1016/j.watres.2020.116003
- Krumbein, W. E., and Altmann, H. J. (1973). A new method for the detection and enumeration of manganese oxidizing and reducing microorganisms. *Helgol. Mar. Res.* 25,347-356. doi: 10.1007/BF01611203
- Kurdi, M. Z., Olichney, J., and Geszvain, K. (2022). A bioinformatic study of the distribution of Mn oxidation proteins in sequenced bacterial genomes. Biorxiv [Preprint]. doi: 10.1101/2022.11.10.515945
- Kurt, H. (2019). "Depth distribution of microbial diversity in lakes" in Freshwater microbiology: Perspectives of bacterial dynamics in Lake ecosystems. eds. S. A. Bandh, S. Shafi and N. Shameem (San Diego, CA: Academic Press), 225–262.
- Lanbroek, H. J., and Bollmann, A. (2011). "Nitrification in inland waters" in Nitrification. eds. B. B. Ward, D. J. Arp and M. G. Klotz (Washington, DC: ASM Press), 385–403.
- LaRowe, D. E., Carlson, H. K., and Amend, J. P. (2021). The energetic potential for undiscovered manganese metabolisms in nature. *Front. Microbiol.* 12:636145. doi: 10.3389/fmicb.2021.636145
- Lau, M. P., Sander, M., Gelbrecht, J., and Hupfer, M. (2016). Spatiotemporal redox dynamics in a freshwater lake sediment under alternating oxygen availabilities: combined analyses of dissolved and particulate electron acceptors. *Environ. Chem.* 13:826. doi: 10.1071/EN15217
- Lenstra, W. K., Klomp, R., Molema, F., Behrends, T., and Slomp, C. P. (2021). A sequential extraction procedure for particulate manganese and its application to coastal marine sediments. *Chem. Geol.* 584:120538. doi: 10.1016/j.chemgeo.2021.120538
- Leu, A. O., Cai, C., McIlroy, S. J., Southam, G., Orphan, V. J., Yuan, Z., et al. (2020). Anaerobic methane oxidation coupled to manganese reduction by members of the Methanoperedenaceae. *ISME J.* 14, 1030–1041. doi: 10.1038/s41396-020-0590-x

Leveque, B., Burnet, J.-B., Dorner, S., and Bichai, F. (2021). Impact of climate change on the vulnerability of drinking water intakes in a northern region. *Sustain. Cities Soc.* 66:102656. doi: 10.1016/j.scs.2020.102656

- Li, N., Huang, T., Mao, X., Zhang, H., Li, K., Wen, G., et al. (2019). Controlling reduced iron and manganese in a drinking water reservoir by hypolimnetic aeration and artificial destratification. *Sci. Total Environ.* 685, 497–507. doi: 10.1016/j.scitotenv.2019.05.445
- Li, G., Su, Y., Wu, B., Han, G., Yu, J., Yang, M., et al. (2022). Initial formation and accumulation of manganese deposits in drinking water pipes: investigating the role of microbial-mediated processes. *Environ. Sci. Technol.* 56, 5497–5507. doi: 10.1021/acs.est.1c08293
- Li, L., and Yang, X. (2018). The essential element manganese, oxidative stress, and metabolic diseases: links and interactions. *Oxidative Med. Cell. Longev.* 2018:7580707. doi: 10.1155/2018/7580707
- Li, D., Zhang, J., Yu, J., and Wang, H. (2024). Synergistic denitrification and Mn cycle driven by sulfur autotrophy significantly enhanced nitrogen removal. *J. Environ. Chem. Eng.* 12:112917. doi: 10.1016/j.jece.2024.112917
- Liu, J., Chen, Q., Yang, Y., Wei, H., Laipan, M., Zhu, R., et al. (2022). Coupled redox cycling of fe and Mn in the environment: the complex interplay of solution species with fe- and Mn-(oxyhydr)oxide crystallization and transformation. *Earth-Sci. Rev.* 232:104105. doi: 10.1016/j.earscirev.2022.104105
- Liu, W., Jiang, H., Yang, J., and Wu, G. (2018). Gammaproteobacterial diversity and carbon utilization in response to salinity in the lakes on the Qinghai–Tibetan plateau *Geomicrobiol J.* 35 392–403 doi: 10.1080/01490451.2017.1378951
- Liu, Y., Wang, Y., Song, X., Hou, X., Cao, X., and Wang, Y. (2023). The evolution of nitrogen transformation microorganism consortium under continued manganese domestication conditions. *Sci. Total Environ.* 899:165656. doi: 10.1016/j.scitotenv.2023.165656
- Liu, W., Xiao, H., Ma, H., Li, Y., Adyel, T. M., and Zhai, J. (2020). Reduction of methane emissions from manganese-rich constructed wetlands: role of manganese-dependent anaerobic methane oxidation. *Chem. Eng. J.* 387:123402. doi: 10.1016/j.cej.2019.123402
- Liu, Q., Yang, J., Wang, B., Liu, W., Hua, Z., and Jiang, H. (2022). Influence of salinity on the diversity and composition of carbohydrate metabolism, nitrogen and sulfur cycling genes in lake surface sediments. *Front. Microbiol.* 13:1019010. doi: 10.3389/fmicb.2022.1019010
- Liu, J., Yao, J., Wang, F., Ni, W., Liu, X., Sunahara, G., et al. (2018). China's most typical nonferrous organic-metal facilities own specific microbial communities. *Sci. Rep.* 8:12570. doi: 10.1038/s41598-018-30519-1
- Louca, S., Parfrey, L. W., and Doebeli, M. (2016). Decoupling function and taxonomy in the global ocean microbiome. *Science* 353, 1272–1277. doi: 10.1126/science.aaf4507
- Lovley, D. R. (1991). Dissimilatory fe(III) and Mn(IV) reduction. *Microbiol. Rev.* 55, 259–287. doi: 10.1128/mr.55.2.259-287.1991
- Lovley, D. R. (1995). Microbial reduction of iron, manganese, and other metals. *Adv. Agron.* 54, 175–231. doi: 10.1016/S0065-2113(08)60900-1
- Lovley, D. R. (2006). "Dissimilatory fe(III)- and Mn(IV)-reducing prokaryotes" in The prokaryotes. eds. M. Dworkin, S. Falkow, E. Rosenberg, K.-H. Schleifer and E. Stackebrandt (New York, NY: Springer), 635–658.
- Lovley, D. R., Giovannoni, S. J., White, D. C., Champine, J. E., Phillips, E. J., Gorby, Y. A., et al. (1993). *Geobacter metallireducens* gen. Nov. sp. nov., a microorganism capable of coupling the complete oxidation of organic compounds to the reduction of iron and other metals. *Arch. Microbiol.* 159, 336–344. doi: 10.1007/BF00290916
- Lovley, D. R., Holmes, D. E., and Nevin, K. P. (2004). "Dissimilatory fe(III) and Mn(IV) reduction" in Advances in microbial physiology. eds. R. K. Pool and D. J. Kelly (London: Academic Press), 219–286.
- Lovley, D. R., and Phillips, E. J. (1988). Novel mode of microbial energy metabolism: organic carbon oxidation coupled to dissimilatory reduction of iron or manganese. *Appl. Environ. Microbiol.* 54, 1472–1480. doi: 10.1128/aem.54.6.1472-1480.1988
- Lovley, D. R., and Phillips, E. J. (1994). Novel processes for anaerobic sulfate production from elemental sulfur by sulfate-reducing bacteria. *Appl. Environ. Microbiol.* 60, 2394–2399. doi: 10.1128/aem.60.7.2394-2399.1994
- Ma, S., Luther, G. W. III, Keller, J., Madison, A. S., Metzger, E., Emerson, D., et al. (2008). Solid-state au/hg microelectrode for the investigation of fe and Mn cycling in a freshwater wetland: implications for methane production. *Electroanalysis* 20, 233–239. doi: 10.1002/elan.200704048
- Ma, D., Wu, J., Yang, P., and Zhu, M. (2020). Coupled manganese redox cycling and organic carbon degradation on mineral surfaces. *Environ. Sci. Technol.* 54, 8801–8810. doi: 10.1021/acs.est.0c02065
- Madison, A. S., Tebo, B. M., Mucci, A., Sundby, B., and Luther, G. W. (2013). Abundant porewater Mn(III) is a major component of the sedimentary redox system. *Science* 341, 875–878. doi: 10.1126/science.1241396
- Mehrani, M.-J., Sobotka, D., Kowal, P., Ciesielski, S., and Makinia, J. (2020). The occurrence and role of Nitrospira in nitrogen removal systems. *Bioresour. Technol.* 303:122936. doi: 10.1016/j.biortech.2020.122936

Miyata, N., Suganuma, R., Sunouchi, K., Okano, K., Fuchida, S., Watanabe, M., et al. (2024). Biological Mn(II) oxidation under organic substrate-limited conditions and its application in mine drainage remediation. *Biochem. Eng. J.* 203:109187. doi: 10.1016/j.bej.2023.109187

- Morgan, J. J. (2005). Kinetics of reaction between O₂ and Mn(II) species in aqueous solutions. *Geochim. Cosmochim. Acta* 69, 35–48. doi: 10.1016/j.gca.2004.06.013
- Munger, Z. W., Carey, C. C., Gerling, A. B., Doubek, J. P., Hamre, K. D., McClure, R. P., et al. (2019). Oxygenation and hydrologic controls on iron and manganese mass budgets in a drinking-water reservoir. *Lake Reserv. Manage* 35, 277–291. doi: 10.1080/10402381.2018.1545811
- Newton, R. J., Jones, S. E., Eiler, A., McMahon, K. D., and Bertilsson, S. (2011). A guide to the natural history of freshwater lake bacteria. *Microbiol. Mol. Biol. Rev.* 75, 14–49. doi: 10.1128/mmbr.00028-10
- Okazaki, M., Sugita, T., Shimizu, M., Ohode, Y., Iwamoto, K., Vrind-de Jong, E. W., et al. (1997). Partial purification and characterization of manganese-oxidizing factors of *Pseudomonas fluorescens* GB-1. *Appl. Environ. Microbiol.* 63, 4793–4799. doi: 10.1128/aem.63.12.4793-4799.1997
- Okita, P. M., and Shanks, W. C. (1992). Origin of stratiform sediment-hosted manganese carbonate ore deposits: examples from Molango, Mexico, and TaoJiang, China. *Chem. Geol.* 99, 139–163. doi: 10.1016/0009-2541(92)90036-5
- Oksanen, J., Simpson, G., Blanchet, F., Kindt, R., Legendre, P., Minchin, P., et al. (2025). Vegan: community ecology Package_. [computer software]. R package version. Available online at: https://CRAN.R-project.org/package=vegan (Accessed April 24, 2025).
- Palomo, A., Jane Fowler, S., Gülay, A., Rasmussen, S., Sicheritz-Ponten, T., and Smets, B. F. (2016). Metagenomic analysis of rapid gravity sand filter microbial communities suggests novel physiology of *Nitrospira* spp. *ISME J.* 10, 2569–2581. doi: 10.1038/ismej.2016.63
- Patrick, W. H., and Henderson, R. E. (1981). Reduction and reoxidation cycles of manganese and iron in flooded soil and in water solution. *Soil Sci. Soc. Am. J.* 45, 855–859. doi: 10.2136/sssaj1981.03615995004500050006x
- Peng, Q., Shaaban, M., Wu, Y., Hu, R., Wang, B., and Wang, J. (2016). The diversity of iron reducing bacteria communities in subtropical paddy soils of China. *Appl. Soil Ecol.* 101, 20–27. doi: 10.1016/j.apsoil.2016.01.012
- Pimenov, N. V., and Neretin, L. N. (2006). "Composition and activities of microbial communities involved in carbon, sulfur, nitrogen and manganese cycling in the oxic/anoxic interface of the Black Sea" in Past and present water column anoxia. ed. L. N. Neretin (Dordrecht: Springer), 501–521.
- Piper, D. Z., Basler, J. R., and Bischoff, J. L. (1984). Oxidation state of marine manganese nodules. *Geochim. Cosmochim. Acta* 48, 2347–2355. doi: 10.1016/0016-7037(84)90230-8
- Poulton, S. W., and Canfield, D. E. (2005). Development of a sequential extraction procedure for iron: implications for iron partitioning in continentally derived particulates. *Chem. Geol.* 214, 209–221. doi: 10.1016/j.chemgeo.2004.09.003
- Pyne, M. E., Bruder, M., Moo-Young, M., Chung, D. A., and Chou, C. P. (2014). Technical guide for genetic advancement of underdeveloped and intractable *clostridium*. *Biotechnol. Adv.* 32, 623–641. doi: 10.1016/j.biotechadv.2014.04.003
- Quast, C., Pruesse, E., Yilmaz, P., Gerken, J., Schweer, T., Yarza, P., et al. (2013). The SILVA ribosomal RNA gene database project: improved data processing and web-based tools. *Nucleic Acids Res.* 41, D590–D596. doi: 10.1093/nar/gks1219
- Sansupa, C., Wahdan, S. F. M., Hossen, S., Disayathanoowat, T., Wubet, T., and Purahong, W. (2021). Can we use functional annotation of prokaryotic taxa (FAPROTAX) to assign the ecological functions of soil bacteria? *Appl. Sci.* 11:688. doi: 10.3390/app11020688
- Schaller, T., and Wehrli, B. (1997). Geochemical-focusing of manganese in lake sediments? An indicator of deep-water oxygen conditions. *Aquat. Geochem.* 2, 359–378. doi: 10.1007/bf00115977
- Scholtysik, G., Dellwig, O., Roeser, P., Arz, H. W., Casper, P., Herzog, C., et al. (2020). Geochemical focusing and sequestration of manganese during eutrophication of Lake Stechlin (NE Germany). *Biogeochemistry* 151, 313–334. doi: 10.1007/s10533-020-00729-9
- Scholtysik, G., Goldhammer, T., Arz, H. W., Moros, M., Littke, R., and Hupfer, M. (2022). Geochemical focusing and burial of sedimentary iron, manganese, and phosphorus during lake eutrophication. *Limnol. Oceanogr.* 67, 768–783. doi: 10.1002/lno.12019
- Schwertmann, U., and Taylor, R. M. (1989). "Iron Oxides" in Minerals in soil environments. eds. J. B. Dixon and S. B. Weed (Madison, WI: Soil Science Society of America), 379–438.
- Sharak Genthner, B. R., and Devereux, R. (2015). "Desulfomicrobium", in Bergey's manual of systematics of archaea and bacteria, eds. Whitman, W. B., Aharal, D. R., Christensen, H., Chuvochina, M., Dedysh, S., Gasparich, G. E., et al. (Hoboken, NJ: Wiley), 1–9.
- Shoiful, A., Kambara, H., Cao, L. T. T., Matsushita, S., Kindaichi, T., Aoi, Y., et al. (2020). Mn(II) oxidation and manganese-oxide reduction on the decolorization of an azo dye. *Int. Biodeterior. Biodegrad.* 146:104820. doi: 10.1016/j.ibiod.2019.104820

- Sikora, A., Detman, A., Chojnacka, A., and Blaszczyk, M. K. (2017). "Anaerobic digestion: I. A common process ensuring energy flow and the circulation of matter in ecosystems. II. A tool for the production of gaseous biofuels" in Fermentation processes. ed. A. F. Jozala (London: InTechOpen), 271–301.
- Silburn, B., Kröger, S., Parker, E. R., Sivyer, D. B., Hicks, N., Powell, C. F., et al. (2017). Benthic pH gradients across a range of shelf sea sediment types linked to sediment characteristics and seasonal variability. *Biogeochemistry* 135, 69–88. doi: 10.1007/s10533-017-0323-z
- Song, T., Tu, W., Chen, S., Fan, M., Jia, L., Wang, B., et al. (2024). Relationships between high-concentration toxic metals in sediment and evolution of microbial community structure and carbon-nitrogen metabolism functions under long-term stress perspective. *Environ. Sci. Pollut. Res. Int.* 31, 29763–29776. doi: 10.1007/s11356-024-33150-y
- Stein, L. Y., La Duc, M. T., Grundl, T. J., and Nealson, K. H. (2001). Bacterial and archaeal populations associated with freshwater ferromanganous micronodules and sediments. *Environ. Microbiol.* 3, 10–18. doi: 10.1046/j.1462-2920.2001.00154.x
- Stenstrom, M. K., and Poduska, R. A. (1980). The effect of dissolved oxygen concentration on nitrification. Water Res. 14, 643–649. doi: 10.1016/0043-1354(80)90122-0
- Su, G., Zopfi, J., Niemann, H., and Lehmann, M. F. (2022). Multiple groups of methanotrophic bacteria mediate methane oxidation in anoxic lake sediments. *Front. Microbiol.* 13:864630. doi: 10.3389/fmicb.2022.864630
- Su, G., Zopfi, J., Yao, H., Steinle, L., Niemann, H., and Lehmann, M. F. (2020). Manganese/iron-supported sulfate-dependent anaerobic oxidation of methane by archaea in lake sediments. *Limnol. Oceanogr.* 65, 863–875. doi: 10.1002/lno.11354
- Sujith, P. P., and Bharathi, P. A. L. (2011). "Manganese oxidation by bacteria: biogeochemical aspects" in Molecular biomineralization: Aquatic organisms forming extraordinary materials. ed. W. E. G. Müller (Berlin: Springer), 49–76.
- Tebo, B. M., Bargar, J. R., Clement, B. G., Dick, G. J., Murray, K. J., Parker, D., et al. (2004). Biogenic manganese oxides: properties and mechanisms of formation. *Annu. Rev. Earth Planet. Sci.* 32, 287–328. doi: 10.1146/annurev.earth.32.101802.120213
- Tebo, B. M., Johnson, H. A., McCarthy, J. K., and Templeton, A. S. (2005). Geomicrobiology of manganese(II) oxidation. *Trends Microbiol.* 13, 421–428. doi: 10.1016/j.tim.2005.07.009
- Thamdrup, B., Rosselló-Mora, R., and Amann, R. (2000). Microbial manganese and sulfate reduction in Black Sea shelf sediments. *Appl. Environ. Microbiol.* 66, 2888–2897. doi: 10.1128/AEM.66.7.2888-2897.2000
- Thevenieau, F., Fardeau, M.-L., Ollivier, B., Joulian, C., and Baena, S. (2007). *Desulfomicrobium thermophilum* sp. nov., a novel thermophilic sulphate-reducing bacterium isolated from a terrestrial hot spring in Colombia. *Extremophiles* 11, 295–303. doi: 10.1007/s00792-006-0039-9
- Tobiason, J. E., Bazilio, A., Goodwill, J., Mai, X., and Nguyen, C. (2016). Manganese removal from drinking water sources. *Curr. Pollut. Rep.* 2, 168–177. doi: 10.1007/s40726-016-0036-2
- Tong, H., Li, J., Chen, M., Fang, Y., Yi, X., Dong, L., et al. (2023). Iron oxidation coupled with nitrate reduction affects the acetate-assimilating microbial community structure elucidated by stable isotope probing in flooded paddy soil. *Soil Biol. Biochem.* 183:109059. doi: 10.1016/j.soilbio.2023.109059
- Vandieken, V., Pester, M., Finke, N., Hyun, J.-H., Friedrich, M. W., Loy, A., et al. (2012). Three manganese oxide-rich marine sediments harbor similar communities of acetate-oxidizing manganese-reducing bacteria. *ISME J.* 6, 2078–2090. doi: 10.1038/ismej.2012.41
- Vigliotta, G., Nutricati, E., Carata, E., Tredici, S. M., de Stefano, M., Pontieri, P., et al. (2007). Clonothrix fusca Roze 1896, a filamentous, sheathed, methanotrophic γ-proteobacterium. Appl. Environ. Microbiol. 73, 3556–3565. doi: 10.1128/AEM.02678-06
- Villemur, R., Lanthier, M., Beaudet, R., and Lépine, F. (2006). The *Desulfitobacterium* genus. *FEMS Microbiol. Rev.* 30, 706–733. doi: 10.1111/j.1574-6976.2006.00029.x
- von Gunten, H. R., Sturm, M., and Moser, R. N. (1997). 200-year record of metals in lake sediments and natural background concentrations. *Environ. Sci. Technol.* 31, 2193–2197. doi: 10.1021/es960616h
- Vuilleumier, S., Nadalig, T., Ul Haque, M. F., Magdelenat, G., Lajus, A., Roselli, S., et al. (2011). Complete genome sequence of the chloromethane-degrading *Hyphomicrobium* sp. strain MC1. *J. Bacteriol.* 193, 5035–5036. doi: 10.1128/JB.05627-11
- Wallenius, A. J., Dalcin Martins, P., Slomp, C. P., and Jetten, M. S. M. (2021). Anthropogenic and environmental constraints on the microbial methane cycle in coastal sediments. *Front. Microbiol.* 12:631621. doi: 10.3389/fmicb.2021.631621

- Wang, K., Jia, R., Li, L., Jiang, R., and Qu, D. (2020). Community structure of *Anaeromyxobacter* in fe(III) reducing enriched cultures of paddy soils. *J. Soils Sediments* 20, 1621–1631. doi: 10.1007/s11368-019-02529-7
- Wang, C., Liu, J., Wang, Z., and Pei, Y. (2014). Nitrification in lake sediment with addition of drinking water treatment residuals. *Water Res.* 56, 234–245. doi: 10.1016/j.watres.2014.03.012
- Wang, X., Xie, G.-J., Tian, N., Dang, C.-C., Cai, C., Ding, J., et al. (2022). Anaerobic microbial manganese oxidation and reduction: a critical review. *Sci. Total Environ.* 822:153513. doi: 10.1016/j.scitotenv.2022.153513
- Wang, Z., Yin, Q., Gu, M., He, K., and Wu, G. (2018). Enhanced azo dye reactive red 2 degradation in anaerobic reactors by dosing conductive material of ferroferric oxide. *J. Hazard. Mater.* 357, 226–234. doi: 10.1016/j.jhazmat.2018.06.005
- Watanabe, M., Tum, S., Katayama, T., Gotore, O., Okano, K., Matsumoto, S., et al. (2024). Accelerated manganese(II) removal by *in situ* mine drainage treatment system without organic substrate amendment: metagenomic insights into chemolithoautotrophic manganese oxidation via extracellular electron transfer. *J. Environ. Chem. Eng.* 12:113314. doi: 10.1016/j.jece.2024.113314
- Wendt-Potthoff, K., Kloß, C., Schultze, M., and Koschorreck, M. (2014). Anaerobic metabolism of two hydro-morphological similar pre-dams under contrasting nutrient loading (Rappbode reservoir system, Germany). *Int. Rev. Hydrobiol.* 99, 350–362. doi: 10.1002/iroh.201301673
- Wickham, H. (2016). "Data analysis" in ggplot2: Elegant graphics for data analysis. ed. H. Wickham (Cham: Springer), 189–201.
- Widdel, F., and Bak, F. (1992). "Gram-negative mesophilic sulfate-reducing bacteria" in The prokaryotes: Prokaryotic physiology and biochemistry. eds. A. Balows, H. G. Trüper, M. Dworkin, W. Harder and K.-H. Schleifer (New York, NY: Springer), 3352–3378.
- Willmitzer, H., Jäschke, K., Berendonk, T., and Paul, L. (2015). Einfluss von Klimaänderungen auf die Wasserqualität von Talsperren und Strategien zur Minimierung der Auswirkungen. DVGW Energie/Wasser-Praxis Available online at: https://www.dvgw.de/medien/dvgw/wasser/klimawandel/einfluss-klimaaenderungenenergie-wasser-praxis-dez-2015.pdf (Accessed July 16, 2025).
- WHO (2021). Manganese in drinking-water background document for development of WHO guidelines for drinking-water quality: WHO/HEP/ECH/WSH/2021.5. Available online at: https://www.who.int/publications/i/item/WHO-HEP-ECH-WSH-2021.5 (Accessed July 16, 2025).
- Wu, H., Li, Y., Zhang, J., Niu, L., Zhang, W., Cai, W., et al. (2017). Sediment bacterial communities in a eutrophic lake influenced by multiple inflow-rivers. *Environ. Sci. Pollut. Res. Int.* 24, 19795–19806. doi: 10.1007/s11356-017-9602-4
- Yang, Y., Li, Y., and Sun, Q. (2014). Archaeal and bacterial communities in acid mine drainage from metal-rich abandoned tailing ponds, Tongling, China. *Trans. Nonferrous Met. Soc. China* 24, 3332–3342. doi: 10.1016/S1003-6326(14)63474-9
- Yu, L., He, D., Yang, L., Rensing, C., Zeng, R. J., and Zhou, S. (2022). Anaerobic methane oxidation coupled to ferrihydrite reduction by *Methanosarcina barkeri. Sci. Total Environ.* 844:157235. doi: 10.1016/j.scitotenv.2022.157235
- Yu, H., and Leadbetter, J. R. (2020). Bacterial chemolithoautotrophy via manganese oxidation. *Nature* 583, 453–458. doi: 10.1038/s41586-020-2468-5
- Zakharova, Y. R., Parfenova, V. V., Granina, L. Z., Kravchenko, O. S., and Zemskaya, T. I. (2010). Distribution of iron- and manganese-oxidizing bacteria in the bottom sediments of Lake Baikal. *Inland Water Biol.* 3, 313–321. doi: 10.1134/s1995082910040036
- Zemskaya, T. I., Bukin, S. V., Lomakina, A. V., and Pavlova, O. N. (2021). Microorganisms in the sediments of Lake Baikal, the deepest and oldest lake in the world. *Microbiology* 90, 298–313. doi: 10.1134/S0026261721030140
- Zhang, D., Li, M., Yang, Y., Yu, H., Xiao, F., Mao, C., et al. (2022). Nitrite and nitrate reduction drive sediment microbial nitrogen cycling in a eutrophic lake. *Water Res.* 220:118637. doi: 10.1016/j.watres.2022.118637
- Zhang, Y., Tang, Y., Qin, Z., Luo, P., Ma, Z., Tan, M., et al. (2019). A novel manganese oxidizing bacterium-*Aeromonas hydrophila* strain DS02: Mn(II) oxidization and biogenic Mn oxides generation. *J. Hazard. Mater.* 367, 539–545. doi: 10.1016/j.jhazmat.2019.01.012
- Zhang, K., Wu, X., Wang, W., Chen, J., Luo, H., Chen, W., et al. (2022). Anaerobic oxidation of methane (AOM) driven by multiple electron acceptors in constructed wetland and the related mechanisms of carbon, nitrogen, sulfur cycles. *Chem. Eng. J.* 433:133663. doi: 10.1016/j.cej.2021.133663
- Zhou, X., Kosaka, K., Nakanishi, T., Welfringer, T., and Itoh, S. (2020). Manganese accumulation on pipe surface in chlorinated drinking water distribution system: contributions of physical and chemical pathways. *Water Res.* 184:116201. doi: 10.1016/j.watres.2020.116201